

Referee comments are *italicized*; authors' responses are in regular (upright) text.

Anonymous Referee #1

General Comments

The paper presents the dynamical and chemical evolution of the 2012/2013 Northern Hemisphere winter stratosphere using satellite observations of trace gases and polar stratospheric clouds (PSC) along with data assimilation produced meteorological fields. In addition to a wide range of polar vortex averaged diagnostics, the study uses trajectory techniques to isolate the chemical evolution of trace gases from transport during the early winter. Satellite observations from Aura MLS (Microwave Limb Sounder) and CALIPSO (Cloud-Aerosol Lidar and Infrared Pathfinder Satellite Observations) provide a detailed view of PSC processing and associated ozone loss. The two vortices produced by the major SSW (Sudden Stratospheric Warming) of January 2013 are tracked separately in terms of both dynamics and trace gas evolution. These C629 results are placed in the context of past Aura and CALIPSO observations including direct comparisons with a non-SSW winter (2010/2011) and a SSW winter (2009/2010).

Overall this is an excellent discussion paper. The writing is clear and concise and the figures provide meticulously detailed documentation of the unique, early winter ozone loss of 2012/2013. New results include not only the record early winter ozone loss but also shows the usefulness of tracking the individual parts of split vortex evolution as each part of the split vortex encounters different conditions of sunlight and dynamics. Especially innovative is the use of trajectories grouped by each part of the split vortex to document the differences in chemical ozone loss in each part. The documentation of the 2013/2013 winter ozone loss and polar processing combined with innovative analysis and diagnostics should interest many ACPD readers.

We thank the referee for their helpful comments. Our responses are interspersed below.

There are two main points that the authors should address more completely:

(1) In several places the authors state that the polar vortex dissipated in mid-February:

Page 4974, Line 22: "...vortex dissipated in mid-February."

Page 4991, Line 12: “...complete dissipation of the vortex by late February.”

Page 5001, Line 18: “...; by mid-February, the vortex became ill-defined...”

Yet, the zonal mean winds at 60N recovered during February and remained strong through March and April. Presumably, the post mid-February vortex edge had weaker EPV and trace gas gradients, however, the vortex still had a relatively strong circulation associated with it (see plots for 2012-2013 available on http://acd-ext.gsfc.nasa.gov/Data_services/met/ann_data.html). The final warming appears to be in April. In mid-February the vortex appears to be reforming, not dissipating.

The distinction here is that the zonal mean view bears very little relation to the confinement of the vortex or its strength as measured by the permeability of its edge (e.g., by PV gradients along the edge). Indeed, in the zonal mean view, the vortex was weakest during January when the two offspring were individually strong and well-isolated – and widely separated, with anticyclones in between going around a latitude circle, such that they “cancelled out” in the zonal mean. In addition, the timing of the recovery depended strongly on altitude, with both westerly zonal mean winds and significant PV gradients along a well-defined vortex edge re-emerging more quickly at higher altitudes. We have added text in the discussion of Figure 6 (thus in the first paragraph of page 4989) saying: “Although the major SSW commenced and the vortex split in early January 2013 (with concurrent reversal of the high latitude zonal mean winds)...” and “Zonal mean winds (not shown) began to increase in February when the reforming vortex was relatively symmetric and pole-centered. The vortex recovered strongly in the middle and upper stratosphere by mid-February, but very weak PV gradients along the edge of the reformed vortex in the lower stratosphere indicate that it was an insignificant transport barrier there at that time.” On page 4991 in the discussion of K_{eff} in Figure 8a, we have changed the wording to “...complete dissipation of the vortex as a significant transport barrier by late February...”. On page 5001, we have changed the wording to “by mid-February, the vortex no longer represented a significant transport barrier.” We hope that these changes clarify the sense in which we are talking about the disappearance of the vortex.

(2) Page 4983, paragraph starting on Line 25, concerning the trajectory calculations:

Using nearly month long trajectories seems problematic as the longer time trajec-

tories should have larger errors than the shorter trajectories. Why not use more frequent initial states and keep the trajectories more equal in length? Results in Morris et al. (1995) show trajectory errors getting larger with time, with large errors after about 15 days. The Morris et al. (1995) time dependence of the error growth (due to input wind uncertainties, for example, their Fig. 4a) seems similar to difference between the trajectories and the MLS observations seen in January in Fig. 13a and b for nitrous oxide. Has the trajectory error for long trajectories been evaluated for 2012/2013? Can some of the difference shown in Fig. 13b be explained by the longer trajectories used for times near the end of January? Would the N₂O descent rates improve with shorter trajectories?

Reference: Morris, G. A. and co-authors, 1995, Trajectory mapping and applications to data from the Upper Atmosphere Research Satellite, J. Geophys. Res., 100, 16491–16505.

Indeed, the uncertainties in the relatively long trajectories are a cause for concern. Manney et al. (2003) did sensitivity tests using varying durations and reinitialization for RT calculations very similar to those presented here, and concluded that calculations using trajectories 20–40 days long were reasonably accurate, depending on the meteorological situation. However, we also did a test reinitializing every 10–12 days for the period presented here, and did not find substantially different results (but did find some difficulties with advecting air from outside the initialization domain into the region of interest, which were exacerbated by frequent reinitialization). We have added a note to this effect to the paragraph ending on line 22 of page 4984. This is an interesting result, as it suggests that in this case the errors in the RT calculations are more closely related to issues with the 3-D motion fields' accuracy in highly disturbed conditions (and possibly limitations in the relatively coarsely resolved MLS data's ability to capture fully the more complex structure under those conditions) rather than directly to errors accumulated over the length of the trajectory calculations. We have added a note to this effect in the discussion of the RT results, in the paragraph ending on line 20 of page 4998.

Minor Points:

(3) In several places the polar vortex is described as being “well-confined” (Page 4974, Line4; Page 4975, Lines 9 and 14; Page 4991, Line 11, Page 5001, Line 12). From context, this appears to be shorthand for describing a vortex with strong, well-defined, sPV and tracer gradients at the vortex edge. That is, the trace gases

are confined within the vortex, not that the vortex itself is confined. However, the phrase “well-confined vortex” could also be interpreted as a small vortex or a vortex that remains confined over a particular region. One solution would be to define a “well-confined vortex” when first used, or alternatively, write out a more complete description of what specifically is meant each time.

We have changed the wording in these instances to more explicitly state the key point (for this paper) of the effectiveness of the vortices as transport barriers, using phrasing such as “effective {or strong} transport barrier” or “within which air remained isolated” at various points.

(4) The abstract gives a good summary of the work, however, it is longer than needed for an abstract and should be edited down to a single paragraph.

The abstract has been condensed substantially and reorganized to address comments from both referees; it is now one paragraph and just over 300 words (down from about 470). The revised abstract is as follows:

“A sudden stratospheric warming (SSW) in early January 2013 caused the Arctic polar vortex to split and temperatures to rapidly rise above the threshold for chlorine activation. However, ozone in the lower stratospheric polar vortex from late December 2012 through early February 2013 reached the lowest values on record for that time of year. Analysis of Aura Microwave Limb Sounder (MLS) trace gas measurements and Cloud-Aerosol Lidar and Infrared Pathfinder Satellite Observations (CALIPSO) polar stratospheric cloud (PSC) data shows that exceptional chemical ozone loss early in the 2012/13 Arctic winter resulted from a unique combination of meteorological conditions associated with the early January 2013 SSW: Unusually low temperatures in December 2012, offspring vortices within which air remained well isolated for nearly a month after the vortex split, and greater than usual vortex sunlight exposure throughout December 2012 and January 2013. Conditions in the two offspring vortices differed substantially, with the one overlying Canada having lower temperatures, lower nitric acid (HNO_3), lower hydrogen chloride, more sunlight exposure/higher ClO in late January, and a later onset of chlorine deactivation than the one overlying Siberia. MLS HNO_3 and CALIPSO data indicate that PSC activity in December 2012 was more extensive and persistent than at that time in any other Arctic winter in the past decade. Chlorine monoxide (ClO, measured by MLS) rose earlier than previously observed and was the largest on record through mid-January 2013. Enhanced vortex ClO persisted until mid-February despite the cessation of

PSC activity when the SSW started. Vortex HNO_3 remained depressed after PSCs had disappeared; passive transport calculations indicate vortex-averaged denitrification of about 4 ppbv. The estimated vortex-averaged chemical ozone loss, $\sim 0.7\text{--}0.8$ ppmv near 500 K (~ 21 km), was the largest December/January loss in the MLS record from 2004/05–2014/15.”

(5) Page 4979, Line 1-2: *The non-standard reference:*

http://gmao.gsfc.nasa.gov/products/documents/GEOS-520_to_5110.pdf can be replaced with:

Molod, A., L. Takacs, M. Suarez and J. Bacmeister, 2014: Development of the GEOS-5 Atmospheric General Circulation Model: Evolution from MERRA to MERRA2. Geosci. Model Dev. Disc., 7, 7575-7617, doi:10.5194/gmdd-7-7575-2014.

The above reference covers the relevant material found in the non-standard reference.

This has been done, thanks for the reference.

(6) Page 4988, Line 7: *Is there an explanation for the very large, off-scale peak of vortex-integrated CALIPSO backscatter in January 2010?*

There was, indeed, a brief period in January 2010 with record high PSC activity and documented synoptic-scale ice PSCs. This is discussed by Pitts et al. (2011) and Dörnbrack et al. (2012), and we have added a sentence to the discussion of Figure 4 describing this.

(7) Page 4992, Line 2: *“...the altitude of the lowest values decreasing gradually through January.” The low HNO_3 values (440-580K) in January are visible, however the altitude decreasing with time is difficult to see in Fig. 9b. Is it very small?*

The altitude of the lowest values decreases from about 530 to 480 K between about 20 December and mid-January. We have revised the text to give this more specific information, with which we believe the reader can more easily pick out the decrease from the plot (we will also request that Figure 9 be made larger in the final published version, which should also make it easier to discern subtle features).

(8) Page 4996, Line 8: Any ideas or speculation of why there was extensive cold air and PSC activity in early December 2012 that played a key role in the early ozone loss?

This is an extremely interesting question, but saying anything beyond speculation about it is well beyond the scope of this paper. Coy and Pawson (2015) show that the 100hPa vertical component of EP flux from early to past mid-December was small (negative on some days/in some wave numbers) and the website provided by this referee shows that values of 45-75N averaged 100hPa heat flux during this period were exceptionally low. We mention in the revised paper that the exceptional cold in much of December 2012 may be related to these unusually low heat fluxes, which suggest unusually little wave propagation into the stratosphere. It is not clear why this question is referenced to Page 4996, line 8, where the evolution of N₂O in January is being discussed. We have added the comment about the low heat fluxes in December 2012 to the discussion of Figure 2, the paragraph ending on line 25 of Page 4986.

(9) Page 5011, Line 30: Unless specific figures or text from earlier versions are being referenced, why not reference only the most recent WMO ozone report?

We checked the references to WMO reports, and found that we could, indeed, cover these by citing only the 2014 report.

(10) Figures 3a, 8c, 8d, 8f: The filled contour colors appear to run off scale at the highest values. If they do, is anything important missing at the high end? In particular would 3a peak more sharply, showing more detailed agreement with Fig. 3b?

The Figure 8 panels do not show any significant structure in the saturated regions. Figure 3a does show some structure in the saturated region, with the plot with an extended color range possibly emphasizing the similarities with Figure 3b more; the revised paper includes this extended color range version of Figure 3.

(11) Figure 10: Are the orbits plotted relative to the vortex edge? Are the orbits nearly the same for 16 and 28 December cases shown?

The zero point on the tracks is the point closest to the pole, at the turnaround of the orbit. The tracks are in very nearly the same positions on the two days. This information has been added to the Figure 10 caption, along with a brief description of the geographic location of those tracks, which cross over Iceland.

Technical Corrections

(12) Page 4979, Line 12: If this is the first mention of a chemical formula in the body of the text, then the chemical formulas should be spelled out as well.

Done. (HNO₃ was already defined in the introduction.)

(13) Page 4980, Footnote: Change “theta surfaces” to “potential temperature surfaces” or “isentropic surfaces”.

Done.

(14) Page 4983, Line 27: “(e.g., WMO, 2007)”: The WMO reports cited in the reference section are for 2006, 2010, and 2014. Please correct the text.

The reports are indeed for 2006, 2010, and 2014, but the 2006 and 2010 reports were published in 2007 and 2011, respectively, and were cited by the year of publication. However, we now cite only the 2014 report (which was published in 2014) as suggested in an earlier comment.

Referee comments are *italicized*; authors' responses are in regular (upright) text.

Anonymous Referee #2

Manney et al. present a study on the Arctic winter 2012/2013, a winter that was characterized by early winter polar processing and strong ozone loss resulting from the combination of unique dynamical conditions associated with a stratospheric warming in January 2013. Large ozone loss was observed during December and January, which was much larger than previously observed during these months. Nitric acid abundances were also among the lowest in the MLS record for the Arctic, indicating that the stratosphere has been denitrified. ClO enhancement during this winter was also much greater than in any other Arctic winter observed by MLS. This shows that this winter was indeed one of the unique winters during the past decade. This study is very interesting and deserves to be published in ACP. I only have the following suggestions for (minor) revisions which should be considered before publication:

We thank the referee for their helpful comments. Our responses are interspersed below.

Specific comments:

Title: You mention ozone loss, but in fact many more processes than just ozone loss during this winter are analyzed (denitrification, chlorine activation etc.). So, I would suggest to change the title slightly to point this out more clearly.

Both “Polar processing” and “ozone loss” are in the title (in fact, “Polar processing” begins it) – we believe “Polar processing” conveys the occurrence of those other processes. We have, however, changed the “short title” for the running head to “Early winter polar processing in 2012/13” to reflect the multiplicity of processes that were taking place.

Abstract: In my opinion, the abstract is too long and too detailed and could be shortened to make it more concise. It takes too long until the authors come to the point why their study is of importance. I wasn't aware that this winter was so special and was quite confused why this winter was analyzed until I reached the end of the abstract. I would suggest to move this sentences higher up, so that they occur rather at the begin of the abstract than at the end.

We have condensed the abstract (per suggestions from both referees) and reorga-

nized it along the lines suggested here; it is now one paragraph and just over 300 words (down from about 470). The revised abstract is as follows:

“A sudden stratospheric warming (SSW) in early January 2013 caused the Arctic polar vortex to split and temperatures to rapidly rise above the threshold for chlorine activation. However, ozone in the lower stratospheric polar vortex from late December 2012 through early February 2013 reached the lowest values on record for that time of year. Analysis of Aura Microwave Limb Sounder (MLS) trace gas measurements and Cloud-Aerosol Lidar and Infrared Pathfinder Satellite Observations (CALIPSO) polar stratospheric cloud (PSC) data shows that exceptional chemical ozone loss early in the 2012/13 Arctic winter resulted from a unique combination of meteorological conditions associated with the early January 2013 SSW: Unusually low temperatures in December 2012, offspring vortices within which air remained well isolated for nearly a month after the vortex split, and greater than usual vortex sunlight exposure throughout December 2012 and January 2013. Conditions in the two offspring vortices differed substantially, with the one overlying Canada having lower temperatures, lower nitric acid (HNO_3), lower hydrogen chloride, more sunlight exposure/higher ClO in late January, and a later onset of chlorine deactivation than the one overlying Siberia. MLS HNO_3 and CALIPSO data indicate that PSC activity in December 2012 was more extensive and persistent than at that time in any other Arctic winter in the past decade. Chlorine monoxide (ClO, measured by MLS) rose earlier than previously observed and was the largest on record through mid-January 2013. Enhanced vortex ClO persisted until mid-February despite the cessation of PSC activity when the SSW started. Vortex HNO_3 remained depressed after PSCs had disappeared; passive transport calculations indicate vortex-averaged denitrification of about 4 ppbv. The estimated vortex-averaged chemical ozone loss, $\sim 0.7\text{--}0.8$ ppmv near 500 K (~ 21 km), was the largest December/January loss in the MLS record from 2004/05–2014/15.”

P4974, L6: Please give a temperature for the chlorine activation threshold.

While we believe this information is important to provide in the text, and the values used as a function of pressure are discussed in the methods section, we feel that adding this interrupts the flow of the abstract, and is more detail than is appropriate for an abstract (particularly when our abstract was already too long and detailed).

P4974, L8: That would mean that the vortex was located quite far in the south.

Can you be more precise? Where exactly was the vortex located. How far south did the vortex reach?

Again, we feel this is detail that, while shown very specifically in the body of the paper (Figure 11), breaks up the flow of and adds to the length of an already long abstract.

P4974, L9-10: In case of MLS first the long name is given and then the abbreviation. In case of CALIPSO it is vice versa. I would suggest to do this consistent throughout the paper, either first the abbreviation and then the long name or vice versa.

All cases have been changed to long name (abbreviation).

P4974, L21: Is 4 ppbv much? Does that mean it was a strong denitrification. I would suggest to point out more clearly what this means.

To our knowledge, the amount of denitrification in the other years discussed here (2009/10 and 2010/11) when it was substantial has not been quantified from observations. It is very difficult to do so, since HNO_3 decreases in winter are typically partly because of temporary sequestration in PSCs, and decreases in late winter to spring result partially from photolysis. In fact, it was the unique situation of denitrification in 2012/13 occurring early and the signal persisting (in the confined offspring vortices) well after there were no longer PSCs, but before photolysis was significant, that allowed straightforward quantification of denitrification. Thus this question is not only too complex to address in the brief summary in the abstract, but is in fact well beyond the scope of the paper itself. We have, however, added a comment on the difficulty of assessing denitrification in the presence of sequestration in PSCs and/or significant photolysis, and thus the inability to compare quantitatively with 2009/10 and 2010/11, on page 4996, around line 13, where we compare qualitatively with those years.

P4974, L1-26: As mentioned above, reading the first paragraph of the abstract without being aware how special this winter was, I did not understand it and was wondering why this study was performed. Of course, I realized that there must have been something special, but I wasn't sure what. The questions that came up in my mind was: What is so special with this winter? Was it the split, the unusual long exposure of the vortex to sunlight or the high chlorine activation?

It was the combination of the vortex split, the exceptional cold in December and

the unusual exposure to sunlight. We believe that the revised abstract shown above clarifies this.

P4974, L28: Please add the CALIPSO observation period.

The duration (so far) of the MLS and CALIPSO observation periods is given in the revised abstract.

P4975, L24-31: As mentioned above I would suggest to move these sentences up.

The abstract has been reorganized as shown above, with this information now near the beginning.

P4975, L26: I would appreciate if also other publications discussing Arctic ozone loss during the 2010/2011 winter would be cited, as e.g. the publications by Sinnhuber et al. (2011), Kuttipurath et al. (2012), Arnone et al. (2012), Hommel et al. (2014).

We have added these references here, as well as the 2014 WMO report (which has numerous other references discussing this winter), along with “and references therein”.

P4977, L24: Same comment as above; first the abbreviation or the long name?

All cases have been changed to long name (abbreviation).

P4978, L10-11: First the abbreviation and then the long name or vice versa as mentioned above.

All cases have been changed to long name (abbreviation).

P4978, L10: Is the usage of the abbreviation G591 for the GEOS data really necessary? I would suggest to just call it GEOS or GEOS-5 (or even GEOS-591 if you prefer to use the version number).

We believe the version number is needed to distinguish it from the GEOS-5.2.0-based MERRA data that we also use/discuss. However, we have changed the references to it to “GEOS-5.9.1”.

P4979, L1-2: The link to the web page could be given as footnote.

This has been replaced with a standard reference suggested by referee 1.

P4981, L16: see my comment on page/line P4978, L10.

See response to that comment.

P4982, L7: As mentioned in one of my previous comment other studies showing the severe ozone loss during the Arctic winter 2010/2011 deserve to be cited as well. Especially, it would be worth to mention the most recent ones as e.g. Hommel et al. (2014) since they usually cite all earlier papers dealing with this winter.

We have added the Hommel et al (2014) citation here, along with the 2014 WMO report and “and references therein”. This and the other suggested references were also added in response to the previous comment.

P4982, L28: The study by Achtert and Tesche (2014) published in JGR should be cited here as well.

This reference has been added as suggested.

P4983-4984: This may be a matter of taste, but I am not very fond of introducing and using too many abbreviations. I do not see any benefit of the abbreviations DMP and LTD, especially since e.g. DMP occurs in the text only twice and LTD only four times.

These names are now spelled out wherever they are used.

P4985, L14-15: “an animation covering...” I would suggest to put this sentence either in brackets or in a footnote.

This has been changed to a parenthetical comment.

P4989, L25 and P4990, L1: As stated above, I am not fond of too many abbreviations. Is the abbreviation VTC really necessary and useful?

This is now spelled out each time it is used.

Section 4: In this section the many different gases and chemical processes are discussed. Wouldn't it be possible to divide this section into subsections to make this section more clearly represented?

We believe showing each view of multiple trace gases together is important to demonstrating the connections between the processes affecting each, so to di-

vide it by trace gases would detract from the message. However, recognizing the length and density of the section, we have divided it into three subsections entitled “Overview and average trace gas evolution” (encompassing descriptions of Figures 7 through 10), “Trace gas evolution in the offspring vortices” (Figure 11 and discussion thereof), and “Comparison with other Arctic winters” (Figure 12 and discussion thereof). We hope that this helps to more clearly focus attention on each of these three key topics in the section.

P4997, L22: What trajectory methods?

We now state “the reverse trajectory and Lagrangian trajectory diagnostic methods described in section 2.3.3” to clarify this.

P4997, L25: What is the abbreviation “RT” standing for? Maybe you introduced it already somewhere in text earlier, but until I came to this paragraph I already have forgotten what it was standing for.

This is spelled out and defined again here, with a reference back to section 2.3.3 where it is first defined.

P5000, L17: The SSW is the cause for the vortex split. This should be clearly stated.

“the vortex-split SSW” has been changed to “an SSW that split the vortex” to clarify this.

P5000, L21: see my comment on page/line P4978, L10.

See response to that comment.

P5002, L17: Please add the MLS observation period considered in this study.

This information has been added.

Technical corrections:

P4994, L 9 and 10: Add “N” so that it reads 60N and 50N, respectively.

Done.

Figure 12 caption: Shouldn't it rather read “for the other Arctic winters...” than “for the other years...”?

Changed as suggested.

Polar processing in a split vortex: early winter Arctic ozone loss in 2012/13

G. L. Manney^{1,2}, Z. D. Lawrence², M. L. Santee³, N. J. Livesey³, A. Lambert³, and M. C. Pitts⁴

¹NorthWest Research Associates, Socorro, NM, USA

²New Mexico Institute of Mining and Technology, Socorro, NM, USA

³Jet Propulsion Laboratory, California Institute of Technology, Pasadena, CA, USA

⁴NASA Langley Research Center, Hampton, VA, USA

Correspondence to: G. L. Manney (manney@nwra.com)

Abstract.

A sudden stratospheric warming (SSW) in early January 2013 caused the [Arctic](#) polar vortex to split. ~~After the lower stratospheric vortex split on 8 January, the two offspring vortices — one over Canada and the other over Siberia — remained intact, well-confined, and largely at latitudes that received sunlight until they reunited at the end of January. As the SSW began, temperatures abruptly rose above chlorine activation thresholds throughout the lower stratosphere. The vortex was very disturbed prior to the SSW, and was exposed to much more sunlight than usual in and~~ [temperatures to rapidly rise above the threshold for chlorine activation. However, ozone in the lower stratospheric polar vortex from late December 2012 and January 2013, through early February 2013 reached the lowest values on record for that time of year. Analysis of Aura Microwave Limb Sounder \(MLS\) ~~nitric acid \(NO₂\) data and observations from CALIPSO \(trace gas measurements and Cloud-Aerosol Lidar and Infrared Pathfinder Satellite Observations \) indicate extensive \(CALIPSO\) polar stratospheric cloud \(PSC\) activity, with evidence of PSCs containing solid nitric acid trihydrate particles during much of December 2012. Consistent with the sunlight exposure and PSC activity, MLS observations show that chlorine monoxide \(ClO\) became enhanced early in December. Despite the cessation of PSC activity with the onset of the SSW, enhanced vortex ClO persisted until mid-February, indicating lingering chlorine activation. The smaller Canadian offspring vortex had data shows that exceptional chemical ozone loss early in the 2012/13 Arctic winter resulted from a unique combination of meteorological conditions associated with the early January 2013 SSW. Unusually low temperatures in December 2012, offspring vortices within which air remained well isolated for nearly a month after the vortex split, and greater than usual vortex sunlight exposure throughout December 2012 and January 2013. Conditions in the two offspring vortices differed~~](#)

substantially, with the one overlying Canada having lower temperatures, lower nitric acid (HNO_3), lower hydrogen chloride (HCl), and, more sunlight exposure/higher ClO in late January than the Siberian vortex. Chlorine deactivation began later in the Canadian than in the Siberian vortex, and a later onset of chlorine deactivation than the one overlying Siberia. MLS HNO_3 and CALIPSO data indicate that PSC activity in December 2012 was more extensive and persistent than at that time in any other Arctic winter in the past decade. Chlorine monoxide (ClO, measured by MLS) rose earlier than previously observed and was the largest on record through mid-January 2013. Enhanced vortex ClO persisted until mid-February despite the cessation of PSC activity when the SSW started. Vortex HNO_3 remained depressed within the vortices after temperatures rose above the PSC existence threshold, and after PSCs had disappeared; passive transport calculations indicate vortex-averaged denitrification of about 4 ppbv; the resulting low values persisted until the vortex dissipated in mid-February. Consistent with the strong chlorine activation and exposure to sunlight, MLS measurements show rapid ozone loss commencing in mid-December and continuing through January. Lagrangian transport estimates suggest. The estimated vortex-averaged chemical ozone loss, $\sim 0.7\text{--}0.8$ ppmv (parts per million by volume) vortex-averaged chemical ozone loss by late January near 500 K ($\sim 21\text{--}21$ km), with substantial loss occurring from ~ 450 to 550 .

The surface area of PSCs in December 2012 was larger than that in any other December observed by CALIPSO. As a result of denitrification, abundances in 2012 was the largest December/13 were among the lowest January loss in the MLS record for the Arctic. ClO enhancement was much greater in December 2012 through mid-January 2013 than that at the corresponding time in any other Arctic winter observed by MLS. Furthermore, reformation of HCl appeared to play a greater role in chlorine deactivation than in more typical Arctic winters. Ozone loss in December 2012 and January 2013 was larger than any previously observed in those months. This pattern of exceptional early winter polar processing and ozone loss resulted from the unique combination of dynamical conditions associated with the early January 2013 SSW, namely unusually low temperatures in December 2012 and offspring vortices that remained well-confined and largely in sunlit regions for about a month after the vortex split. from 2004/05–2014/15.

50 1 Introduction

The Arctic winter stratosphere exhibits extreme interannual variability in dynamical conditions. Because chlorine-catalyzed chemical ozone loss in the polar winter lower stratosphere depends strongly on temperatures and vortex confinement (e.g., Schoeberl et al., 1992; Solomon, 1999), the varying meteorological environment is reflected in large variations in ozone loss. Sudden stratospheric warmings (SSWs) in the Arctic cause temperatures to rise abruptly and the westerly winter circulation to reverse to easterly; they are one of the predominant drivers of Arctic winter variability (e.g., Charlton and Polvani, 2007; Charlton-Perez et al., 2008, and references therein). During “major” SSWs

(SSWs in which the zonal mean zonal winds at 10 hPa reverse from westerly to easterly poleward of 60°), lower stratospheric temperatures usually rise rapidly above the threshold for conversion of chlorine to “active” (ozone-destroying) forms (e.g., Manney et al., 2005; Kuttippurath et al., 2010; Kuttippurath and Nikulin, 2012). The period with conditions conducive to chlorine activation in the Arctic ranges from a few days (in winters with strong SSWs in December, e.g., Manney et al., 1999a, 2005) to over four months (in the exceptional 2010/11 winter, e.g., Manney et al., 2011; Sinnhuber et al., 2011; Arnone et al., 2012; Kuttippurath et al., 2012; Hommel et al., 2014; WMO, 2014; and references therein). In contrast, major SSWs are very rare in the Antarctic and conditions favorable for chemical ozone loss persist from mid-May to mid-October with small interannual variations (WMO, 2014, and references therein).

The reactions that destroy ozone in the polar lower stratosphere also require sunlight (e.g., Solomon, 1999, and references therein). Since a large fraction of the polar vortex is typically in darkness in December and January, early winter ozone loss tends to be small. Consequently, major SSWs in early winter are generally associated with minimal ozone loss through the winters in which they occur. Even among years with comparably extreme SSWs, however, dynamical conditions and ozone loss show large variability. Significant ozone loss has been reported before the major SSWs in late January in 2003 (e.g., Singleton et al., 2005) and 2010 (e.g., Wohltmann et al., 2013). The 2009/10 winter was unusually warm until after mid-December, but unusually cold in January, with temperatures below the ice frost point (~ 188 K near 50 hPa) on synoptic scales from ~ 15 –25 January. This resulted in formation of polar stratospheric clouds (PSCs) with solid nitric acid (HNO_3)-containing particles that were large enough to sediment out, leading to denitrification and a consequent slowing of chlorine deactivation after the late January SSW (e.g., Pitts et al., 2011; Dörnbrack et al., 2012; Khosrawi et al., 2011; Wohltmann et al., 2013). Wohltmann et al. (2013) showed that ozone loss continued, albeit at a decreased rate, for more than a month after temperatures rose above the chlorine activation threshold. Similarly, in 2002/03, the early winter was unusually cold, but the PSC season was terminated by SSWs starting in late January. Chemical ozone loss, which began in late December before the SSW, was facilitated by the disturbed vortex being exposed to more sunlight than usual in December/January (e.g., Singleton et al., 2005). Several studies have shown evidence for Arctic ozone loss in some winters in late December and January up to ~ 0.6 ppmv over shallow layers in the lower stratosphere, but in most winters it is limited to less than ~ 0.3 ppmv (e.g., Manney et al., 2003; Rex et al., 2003; Kuttippurath et al., 2010). Kuttippurath et al. (2010) noted significant ozone loss in late December and early January prior to the late January SSWs in 2006, 2009 and 2010; in 2006 and 2009, the lower stratospheric vortex broke up within one to two weeks after the SSW, resulting in rapid mixing, chlorine deactivation, and abrupt cessation of ozone loss. MLS observations during the 2011/12 winter indicate early chlorine activation and suggest a small amount of ozone loss prior to the January 2012 SSW (Bernhard et al., 2012; WMO, 2014).

An exceptionally strong major SSW occurred in early January 2013. The criteria for a major SSW
95 were first met on 6 January 2013, with a large amplification of wave 2 activity (e.g., Goncharenko
et al., 2013; Coy and Pawson, 2015); the vortex split in the middle stratosphere within 1–2 days
after that time (the timing of the split depends on altitude and on the exact definition of the vortex
edge). Coy and Pawson (2015) showed large wave-2 flux into the stratosphere preceding the event,
and midstratospheric temperatures increasing by 40 K between 1 and 5 January 2013; this upward
100 wave activity flux was associated with Pacific blocking.

Because radiative time scales are long in the lower stratosphere, recovery from prolonged SSWs
such as the 2010 and 2013 events is very slow at the levels where polar processing occurs (e.g. Hitch-
cock and Shepherd, 2013; Hitchcock et al., 2013). Hence, such SSWs typically result in termination
of lower stratospheric polar processing. However, the aforementioned studies of the 2009/10 winter
105 indicate that prolonged SSWs starting in late January may be preceded by significant ozone loss.

In this paper, we examine in detail the evolution of the lower stratospheric polar vortex during
the 2012/13 winter by characterizing the separated offspring vortices following the split during the
January SSW. We combine this information with trace gas data from the Microwave Limb Sounder
(MLS) instrument on NASA’s Aura satellite and information on PSC composition from the Cloud-
110 Aerosol Lidar with Orthogonal Polarization (CALIOP) instrument on NASA’s ~~CALIPSO~~ (Cloud-
Aerosol Lidar and Infrared Pathfinder Satellite Observations ([CALIPSO](#))) satellite to show the pro-
gression of polar processing in the 2012/13 winter and to estimate chemical ozone loss. We compare
polar processing during the 2012/13 winter with that during the other nine Arctic winters observed
so far by Aura MLS and seven observed by CALIPSO, and detail the conditions associated with the
115 early January SSW that led to unexpectedly large early winter ozone loss.

In Sect. 2, we describe the datasets and methods used. Section 3 comprises a detailed discussion
of lower stratospheric vortex and temperature evolution in 2012/13 and the implications of that
evolution for PSC composition. The evolution of trace gases observed by MLS in relation to the
polar vortex is described in Sect. 4. We use trajectory methods to estimate chemical loss and to
120 compare with similar estimates for other winters (Sect. 5). Our conclusions are presented in Sect. 6.

2 Data and methods

2.1 Meteorological data: GMAO analyses

We use data produced by NASA’s Global Modeling and Assimilation Office (GMAO) from their
operational Goddard Earth Observing System (GEOS) version 5.9.1 (~~G591~~[GEOS-5.9.1](#)) analysis
125 and their GEOS version 5.2.0-based ~~MERRA~~ (Modern Era Retrospective Analysis for Research and
Applications ([MERRA](#))) reanalysis. These datasets are from global atmospheric models that com-
bine 3-D-Var assimilation and Incremental Analysis Update (IAU) (Bloom et al., 1996) to constrain
the analyses. Both MERRA and ~~G591~~[GEOS-5.9.1](#) use a hybrid sigma-pressure vertical coordi-

nate with 72 model levels from the surface to 0.01 hPa, and have vertical resolutions of ~ 1 km
130 in the lower stratosphere. These two datasets have slightly different horizontal resolutions: ~~G591~~
[GEOS-5.9.1](#) uses a $0.5^\circ \times 0.625^\circ$ latitude/longitude grid (361×576 gridpoints), while MERRA uses
a $0.5^\circ \times 0.667^\circ$ latitude/longitude grid (361×540 gridpoints). The meteorological fields from these
datasets on their model levels are available eight times per day for ~~G591~~[GEOS-5.9.1](#) (00:00, 03:00,
06:00, 9:00, 12:00, 15:00, 18:00, and 21:00 UT), and four times per day for MERRA (00:00, 06:00,
135 12:00, and 18:00 UT). Potential vorticity (PV) data from MERRA are available only on a reduced
 $1^\circ \times 1.25^\circ$ latitude/longitude grid (181×288 gridpoints) with 42 pressure levels; we interpolate
MERRA PV to match the model levels and grid. Rienecker et al. (2008) and Rienecker et al. (2011)
provide further details about GEOS and MERRA. The differences between GEOS-5.2.0 and GEOS-
5.9.1 are outlined ~~in a document maintained by GMAO at~~ [by](#) Molod et al. (2014).

140 2.2 MLS and CALIPSO data

The Earth Observing System (EOS) Aura and CALIPSO satellites are components of the “A-Train”
constellation, with 98° inclination orbits that provide data coverage from 82° S to 82° N latitude on
every orbit.

Aura was launched in July 2004. Aura MLS measures millimeter- and submillimeter-wavelength
145 thermal emission from the limb of Earth’s atmosphere. Detailed information on the measurement
technique and the Aura MLS instrument is given by Waters et al. (2006). Vertical profiles are mea-
sured every 165 km along the suborbital track and have a horizontal resolution of ~ 200 – 500 km
along-track and a footprint of ~ 3 – 9 km across-track. In this study we use version 3 (v3) Aura MLS
[nitrous oxide \(N₂O\)](#), [HNO₃](#), ~~HCl, ClO,~~ [and hydrogen chloride \(HCl\), chlorine monoxide \(ClO\), and](#)
150 [ozone \(O₃\)](#) measurements from 2004 through 2014. The quality of these data is described by Livesey
et al. (2013). Vertical resolution is about 2.5 km for O₃, 3 km for HCl and ClO, 3–5 km for HNO₃,
and 4–6 km for N₂O in the lower to middle stratosphere. Single-profile precisions are approximately
0.04–0.1 ppmv, 0.2–0.3 ppbv (parts per billion by volume), 0.1 ppbv, 0.7 ppbv, and 13–20 ppbv
for O₃, HCl, ClO, HNO₃, and N₂O, respectively. The v3 MLS data are quality-screened as recom-
155 mended by Livesey et al. (2013), including application of an altitude- and latitude-dependent bias
correction for ClO at 68, 100, and 147 hPa.

The CALIPSO satellite was launched in April 2006. CALIOP, the primary instrument on
CALIPSO, is a lidar that measures backscatter at wavelengths of 1064 and 532 nm, with the 532 nm
signal separated into orthogonal components parallel and perpendicular to the polarization plane of
160 the outgoing laser beam (Winker et al., 2009; Hunt et al., 2009). Multiple scattering can complicate
the analysis of optically thick clouds, but this is not an issue for thin PSCs. On-board data processing
is used to average single-shot samples over specific height ranges. The 532 nm CALIOP calibration
is performed over 11 contiguous 5 km samples in the region 30–34 km, where Rayleigh molec-
ular scattering is assumed. The calibrated data products derived from the three CALIOP channels

165 (Hostetler et al., 2006; Hunt et al., 2009) are attenuated volume backscatter coefficients ($\text{km}^{-1} \text{sr}^{-1}$) as a function of altitude.

2.3 Methods

2.3.1 Dynamical characterization of the polar vortex

Part of our study of the Arctic 2012/13 winter uses diagnostics for assessing meteorological conditions favoring development of PSCs and activation of chlorine. Temperature diagnostics include 170 minimum temperatures, as well as the area (A_{PSC}) and volume (V_{PSC}) of air with temperatures below the threshold ($T \leq T_{\text{PSC}}$) for PSC existence or chlorine activation (note that the subscript “PSC” may be replaced by a specific PSC type). Some recent studies have suggested that liquid PSCs play a dominant role in activating chlorine (e.g., Drdla and Müller, 2012; Wegner et al., 2012; Wohltmann et al., 2013). However, the existence temperatures for solid nitric acid trihydrate (NAT) (Hanson and Mauersberger, 1988) and ice particles remain convenient thresholds for the initiation of chlorine 175 activation processes, and are pertinent to the formation of the solid-particle PSCs discussed here; we thus adopt the convention of referring to T_{NAT} in general discussion related to the possibility of chlorine activation. Polar vortex diagnostics include the area and volume of the polar vortex (A_{Vort} and V_{Vort} , respectively), the sunlit area of the polar vortex (sunlit vortex area, SVA), and maximum PV gradients. We calculate these diagnostics from MERRA data, once per day at 12:00 UT, on potential temperature surfaces ranging from 390 to 580 K (about 14 to 24 km^1), as in Lawrence et al. (2014). More detailed descriptions of these polar processing diagnostics and their use can be found in Manney et al. (2011) and Lawrence et al. (2014).

185 Our characterization of the 2012/13 split polar vortex consists of information about the locations, sizes, and shapes of the individual offspring vortices throughout the stratosphere. We adapted algorithms from image processing to identify and track the vortices through time. We define the vortex edge throughout the stratosphere (25 vertical levels between 390 and 1800 K, ~ 14 –54 km) based on climatological profiles of scaled PV (sPV, e.g., Dunkerton and Delisi, 1986; Manney et al., 1994b) 190 at the location of the maximum PV gradient from MERRA. After identifying closed sPV contours at a single timestep, we reject those with equivalent latitude (EqL, the latitude enclosing the same area between it and the pole as a given contour of PV, Butchart and Remsberg, 1986) greater than 82° , corresponding to areas less than $\sim 1\%$ of a hemisphere. We save the position and extent of each individual vortex in the model grid coordinates, and calculate its 2-D moment diagnostics (e.g., 195 Mitchell et al., 2011), its total and sunlit area, and its concentricity with any existing cold regions (e.g., Lawrence et al., 2014). After identifying the vortex regions, a matching procedure philosophically similar to that used by Limbach et al. (2012) is used to track each offspring vortex through time. This tracking is done using the full time resolution available (8 times per day for [G591-GEOS-5.9.1](#)

¹In polar winter; the altitude of [theta-isentropic](#) surfaces in the lower stratosphere is higher by 1–2 km in December 2012 than in January 2013.

and 4 times per day for MERRA) to maximize its accuracy. The multiple vortex characterization
200 procedures and additional applications are described in detail by Lawrence and Manney (2015).

In addition to the diagnostics of polar chemical processing described above, effective diffusivity
(K_{eff}) is calculated from PV as a diagnostic of mixing. K_{eff} is expressed as log-normalized equivalent
length, that is, the length of a tracer contour with respect to the contour of minimum length that would
enclose the same area; high (low) values thus reflect complex (simple) structure in tracer (here PV)
205 contours and indicate strong (weak) mixing (e.g., Nakamura, 1996; Haynes and Shuckburgh, 2000;
Allen and Nakamura, 2001). The magnitudes of K_{eff} values depend strongly on the resolution of
the tracer fields used in the calculations, but values from MERRA and ~~G591~~ [GEOS-5.9.1](#) agree
qualitatively; ~~G591~~ [GEOS-5.9.1](#) values are shown here.

To place the 2012/13 winter in the context of other Arctic winters, in addition to comparing with
210 the 35 year MERRA reanalysis, we compare vortex and temperature diagnostics for that winter with
those for 2009/10 (a year during the Aura and CALIPSO missions for which low temperatures, ex-
tensive PSC activity, and large early winter ozone loss before a prolonged SSW have been reported,
e.g., Kuttippurath et al., 2010; Pitts et al., 2011) and 2010/11 ~~-(the year with the most prolonged
[cold period and largest Arctic ozone loss on record, e.g.,](#) Manney et al., 2011; Hommel et al., 2014;
215 WMO, 2014; [and references therein](#)).~~ The interannual variability in the diagnostics shown here is
much larger than any biases between different reanalyses (Lawrence et al., 2014); the results are thus
robust across different meteorological datasets.

2.3.2 CALIPSO PSC classification

The CALIPSO PSC data products are derived from the CALIPSO Lidar Level 1B data products using
220 the PSC detection and composition classification algorithm described in Pitts et al. (2009). The PSC
data product contains profiles of PSC presence, composition, optical properties, and meteorologi-
cal information along CALIPSO orbit tracks reported on a 5 km horizontal by 180 m vertical grid.
PSCs are classified by composition using the CALIPSO PSC algorithm, as described by, e.g., Pitts
et al. (2009, 2011) and Lambert et al. (2012). The classification is based on the measured CALIOP
225 aerosol depolarization and inverse scattering ratios. CALIPSO PSCs are separated into six composi-
tion classes: supercooled ternary solutions (STS), which also include low number densities of NAT
particles whose optical signature is masked by the much more numerous STS droplets at low tem-
peratures; three classes of liquid/NAT mixtures, with MIX1, MIX2, and MIX2-enhanced (MIX2E)
denoting increasingly higher NAT number density/volume; water ice (ICE); and mountain wave ice
230 (WAVE), a subset of ice PSCs generated through strong cooling associated with orographic waves
producing high ice particle number densities ($\sim 10 \text{ cm}^{-3}$) but relatively small (1.0–1.5 μm radius)
particles (e.g., Fueglistaler et al., 2003). ~~An evaluation~~ [Evaluations](#) of the accuracy of the CALIOP
PSC composition classification ~~is~~ [are](#) provided by Pitts et al. (2013) ~~and~~ [Achttert and Tesche \(2014\).](#)

235 A relevant parameter for chlorine activation is the total PSC particle surface area, which is primarily that of spherical liquid PSC particles. The lidar particulate backscatter is the integral over the size distribution of particle geometric cross-section (which is equal to the surface area/4 for spheres) weighted by the Mie backscatter efficiency (Gobbi, 1995). Thus, the summation of CALIOP particulate backscatter within the vortex is proportional to the total PSC particle surface area (which is primarily determined by liquid particles) in that region.

240 2.3.3 MLS data analysis and chemical ozone loss estimates

EqL, sPV, and reanalysis temperatures at the MLS locations are obtained from the MLS derived meteorological products (Manney et al., 2007). MLS data are interpolated to isentropic surfaces using temperatures from MERRA. For daily maps and reverse trajectory initialization (see below) the MLS data are gridded at 2° latitude by 5° longitude using a weighted average around each gridpoint
245 of 24 h of data centered at 12:00 UT. EqL time series are produced using a weighted average of MLS data in EqL, time, and uncertainty (e.g., Manney et al., 1999b, 2007). The vortex average cross-sections shown use a single sPV contour of $1.4 \times 10^{-4} \text{ s}^{-1}$ as a proxy for the vortex edge, while more detailed single-level individual vortex calculations use the altitude-dependent sPV profile described above (Sect. 2.3.1). For averages in multiple vortices, the sPV from the ~~DMPs-derived~~
250 meteorological products is first used to determine whether the MLS measurement location is within any vortex. Those points that are within a vortex are then marked with the labels for individual regions to identify which of multiple vortices they are inside. Averaging improves MLS precisions to values smaller by a factor of about 10 and 100 for EqL means and vortex averages, respectively, over the single-profile precisions listed in Sect. 2.2.

255 The passive subtraction method using “Reverse Trajectory” (RT) calculations originated by Manney et al. (1995a, b) has been used in numerous studies of ozone loss in individual winters, and to characterize interannual variability in ozone loss during the Upper Atmosphere Research Satellite mission (Manney et al., 2003, and references therein). Here, daily 3-D gridded fields of passively transported O_3 , N_2O , and HNO_3 during December 2012 and January 2013 are compared with MLS
260 observations. To the extent that the transport is accurately modeled, the differences between the passively advected and the MLS fields represent the non-transport processes affecting the trace gases – that is, chemical processing and/or, for HNO_3 , microphysical processes and gravitational settling (denitrification) of PSC particles. The calculations for N_2O are used to assess the accuracy of the modeled transport, as per Manney et al. (1995b). The trajectory runs for the RT ozone loss
265 calculations are done using an adapted version of the Lagrangian Trajectory Diagnostic (~~LTD~~) code described by Livesey (2013), which advects parcels using a fourth-order Runge–Kutta scheme. We use winds, temperatures, and diabatic heating rates from MERRA, and perform backward trajectories for days in December 2012 and January 2013. Parcels are initialized on 10 isentropic surfaces from 390 to 660 K (~ 14 – 27 km) on a $2^\circ \times 5^\circ$ Northern Hemisphere latitude/longitude grid. Although every

270 15 min integration timestep is saved, we use only the 12:00 UT locations to determine the estimates
of ozone loss. Passive ozone on the initial grid is obtained by initializing the back trajectories on
a common date. For example, trajectories on each day from 8 December through 1 January were ini-
tialized with gridded MLS data on 8 December to estimate chemical loss on each day of that period.
275 [While Morris et al. \(1995\) found that trajectory errors often increased substantially after about 15
days, Manney et al. \(2003\) found that RT calculations similar to those done here were reasonably
accurate using trajectories 20–40 days long, depending on the meteorological situation.](#) To obtain
estimates for early December through January, while limiting the duration of back trajectories to
no more than a month, the parcels run back from January days are initialized using the results for
1 January from the calculation initialized with MLS data on 8 December. [Sensitivity tests for the
280 8 December 2012 to 31 January 2013 period using trajectories reinitialized every 10–12 days did
not show significantly different results than those presented with a single reinitialization near the
middle of the period. Frequent reinitialization also becomes problematic because air from outside
the initialization domain advected into the region of interest can result in growing areas of missing
data.](#)

285 A different Lagrangian method, the Match-based approach of Livesey et al. (2015), has also been
used to estimate December through January O₃ loss in 2004/05 through 2012/13. The trajectory cal-
culations, or “MLS [LFDsLagrangian trajectory diagnostics](#)”, are described by Livesey (2013) and
the MLS Match method is discussed in detail by Livesey et al. (2015). Briefly, the [LFDsLagrangian
trajectory diagnostics](#) are computed by launching a cluster of parcels from each MLS measure-
290 ment location and time. Airmasses sampled by MLS on multiple orbits are identified using these
[LFDsLagrangian trajectory diagnostics](#), and the differences between ozone at the initial time and
subsequent measurements are used to calculate chemical ozone loss rates in a procedure similar to
that developed by von der Gathen et al. (1995) and Rex et al. (1998, 1999, 2002). Several criteria –
including sPV greater than $1.4 \times 10^{-4} \text{ s}^{-1}$ (indicating vortex air), approximate conservation of sPV,
295 and limited dispersion among the cluster of parcels launched at each location – provide information
to screen the matches. Calculations are done using a “standard” (25 %) and “stricter” (10 %) limit
on the divergence in sPV between matched observations (Livesey et al., 2015). Non-zero changes in
N₂O between matched observations are assumed to arise from errors in modeled transport and are
used to estimate the effect of those errors on O₃ loss uncertainties. In contrast to the sonde-based
300 Match studies with 100s of matches over the course of a winter, the MLS sampling provides 1000s
of matches each day.

3 Polar vortex, temperature and PSC evolution in 2012/13

Figure 1 gives a qualitative overview of the vortex and temperature evolution during the 2012/13
Arctic winter [;\(an animation covering the full winter is available as a Supplement\)](#). A near-split of

305 the lower stratospheric vortex at the beginning of December was associated with a brief temperature
increase. Another vortex split in the lower stratosphere was seen around 10 December. Despite these
significant vortex disturbances, a large, deep region of temperatures below T_{NAT} persisted through
December. By 1 January, a separate cold region developed at high altitude (from about 650 to above
800 K) and merged with the large lower-stratospheric cold region that extended below 390 K. The
310 vortex was often elongated, and the cold region was typically shifted towards the side extending over
North America, especially in the period immediately preceding the early January split associated
with the major SSW, when the vortex was stretched into two (connected) lobes such that the air in the
core of each circulated within that individual lobe. By 4 January, the cold region was much smaller,
though still extending through the depth of the lower stratosphere. During 4 through 6 January the
315 vortex continued to elongate, and temperatures increased above T_{NAT} (Supplement). On 7 January
(shown in Fig. 1), a small region of temperatures below T_{NAT} reappeared at 600 to 750 K. At this
time, the vortex was clearly beginning to split throughout the vertical domain shown.

By 9 January, the vortex was completely split at all levels shown, and no temperatures below
 T_{NAT} remained. Both the simultaneous splitting over a deep altitude region and the unequal split
320 into smaller “Canadian” and larger “Siberian” offspring vortices with positions similar to those in
2012/13 are common characteristics of vortex-split type SSWs (e.g., Matthewman et al., 2009). The
two offspring vortices continued to evolve and remained well-defined throughout the vertical domain
until the last few days of January, with a brief reappearance of temperatures below the activation
threshold between 14 and 18 January (Fig. 1 shows 15 January) in the Canadian vortex. On 26 Jan-
325 uary, the vortices began moving back together, and they merged by 30 January. We describe below
the impact of this temperature and vortex evolution on the potential for polar chemical processing
and O_3 loss.

Figure 2 shows the evolution of lower stratospheric temperatures at 490 K (~ 55 hPa, ~ 20 –
21 km) from the 35 year MERRA reanalysis, with 2009/10, 2010/11, and 2012/13 highlighted.
330 Minimum temperatures (top panel) were unusually low during late November and December 2012
(orange line), but within the range seen in the past 35 years; temperatures below the ice PSC ex-
istence threshold ($T \leq T_{\text{ice}}$) were seen continuously at this level from about 5 December through
1 January. The brief warming associated with the early December lower stratospheric vortex split
resulted in temperatures rising near T_{NAT} at 490 K and above it at lower levels (not shown). The
335 490 K temperatures in December 2012 were much lower than those in December 2009 (which was
unusually warm, e.g., Dörnbrack et al., 2012), and more persistently low than those in Decem-
ber 2011. [Heat fluxes at 100 hPa from approximately 5–20 December 2013 were exceptionally low
\(even negative on some days\)](http://acd-ext.gsfc.nasa.gov/Data_services/met/ann_data.html) (e.g., Coy and Pawson, 2015, also see plots available at [http://acd-
ext.gsfc.nasa.gov/Data_services/met/ann_data.html](http://acd-ext.gsfc.nasa.gov/Data_services/met/ann_data.html)), [a condition often associated with less wave
340 activity and lower temperatures.](http://acd-ext.gsfc.nasa.gov/Data_services/met/ann_data.html)

Temperatures at 490 K in 2012/13 began rising precipitously on 31 December, exceeding T_{NAT} on 5 January 2013. Temperatures dropped to just below T_{NAT} around 13 January, before rising abruptly again starting around 19 January. Minimum temperatures in early January 2013 exceeded T_{NAT} slightly before the onset of the major SSW (that is, the date when the criteria for a major SSW were first met). In contrast, in late January 2010, despite a rapid temperature increase following the onset of the SSW, temperatures remained below T_{NAT} for about a week before gradually rising above that threshold. The late January 2010 SSW was a vortex displacement event, as opposed to a vortex split in 2013 (e.g., Dörnbrack et al., 2012; Coy and Pawson, 2015); previous studies have indicated that vortex split SSWs tend to be more barotropic in the sense of occurring simultaneously over a wide range of altitudes, rather than earlier at higher levels (e.g., Matthewman et al., 2009).

The fraction of the vortex volume with $T \leq T_{\text{NAT}}$, $V_{\text{NAT}}/V_{\text{vort}}$, in 2012/13 (Fig. 2b) was as large as – sometimes slightly larger than – that previously observed in the Arctic both in late November, and, after a brief warming, through the rest of December. The abrupt drop of $V_{\text{NAT}}/V_{\text{vort}}$ to near zero indicates the concurrent disappearance of $T \leq T_{\text{NAT}}$ at all altitudes. This is shown explicitly in Fig. 3a: a large area of $T \leq T_{\text{NAT}}$ formed in late November, with a brief warming in early December; the large area of $T \leq T_{\text{NAT}}$ extended from about 420 to 700 K from about 5 December through the beginning of January, then dropped to zero by 6 January at all levels. There was a brief dip to $T \leq T_{\text{NAT}}$ for a few days in mid-January 2013 at levels between ~ 500 and 600 K. The contrast with the warming associated with the 2010 SSW is seen clearly in the overlaid purple line on Fig. 3a, which drops rapidly above about 520 K (though not as rapidly as in 2013, and after, rather than before, the SSW onset), but much more slowly below that level. Both the 2009/10 and 2010/11 Arctic winters were notable for an unusually deep region of low temperatures (e.g., Manney et al., 2011; Dörnbrack et al., 2012). Figure 3a shows that the cold region in early winter 2012/13 was as deep as that in those two previous winters; this, along with unusually low temperatures during most of December, resulted in the record high $V_{\text{NAT}}/V_{\text{vort}}$.

Figure 3b shows the total area of PSCs detected by CALIPSO. Consistent with the very low temperatures in the last three weeks of December, an extensive area of PSCs was seen from about 17 to 25 km (approximately 430 to 600 K). The volume of various PSC types (Fig. 3c) shows, in addition to a large volume of liquid PSCs, substantial regions of MIX1, MIX2, and MIX2E PSCs during approximately the last three weeks of December, as well as a small region of ice PSCs in mid-December associated with orographic wave activity near Novaya Zemlya (in the Arctic Ocean north of Russia). The widespread presence of these liquid/NAT mixtures, which include large HNO_3 -containing particles, suggests conditions favorable for sedimentation of PSCs and hence denitrification.

As seen in Fig. 4, the vortex-integrated particulate backscatter at 490 K (near 21 km in December 2012) in December in 2012 was as large as or larger than that in the other years (2006 through 2013) observed by CALIPSO, and much larger than the average values during December. The patterns shown here are consistent with the evolution of $V_{\text{NAT}}/V_{\text{vort}}$ (Fig. 2b). None of the other winters

observed had such a persistent period of large vortex-integrated backscatter in December (values: Values in December 2011 define the envelope for the years not shown individually between about 5
380 and 20 December, with much less persistent high values in the other years); the large, off-scale peak
in January 2010 was when CALIPSO observed synoptic-scale ice PSC activity in the exceptionally
cold period before the late January 2010 SSW (e.g., Pitts et al., 2011; Dörnbrack et al., 2012). Since
the vortex-integrated backscatter is a proxy for the total particle surface area, this leads the pervasive
high values in December 2012 lead to the expectation of early chlorine activation.

385 The impact of the temperature evolution described above on the polar processing potential over
the 2012/13 winter in relation to other years is shown in Fig. 5. The total number of days in a winter
with temperatures below T_{NAT} integrated from 390 to 550 K (Fig. 5a) is closely correlated with the
timing of SSWs: major SSWs in 1984/85, 1998/99 and 2001/02 began in December (e.g., Randel
and Boville, 1987; Manney et al., 1999a; Naujokat et al., 2002), and the onset of the major SSW
390 in 2003/04 was in the first few days of January (e.g., Manney et al., 2005). The total number of
cold days in 2012/13 was slightly larger than that in 2003/04 (when the SSW was at a similar time)
because of the unusually deep cold region in 2012/13. Winter mean (1 December through 15 April)
 $V_{\text{NAT}}/V_{\text{vort}}$ (Fig. 5b) shows a considerably larger activation potential in 2012/13 than in the previous
winters with very early SSWs, reflecting the persistent deep cold region in December 2012. Winter
395 mean $V_{\text{NAT}}/V_{\text{vort}}$ was nearly as large as that in 2008/09 and 2009/10, when the major SSWs were
18–20 days later.

Polar vortex characteristics relevant to chemical processing are shown in Fig. 6. Figure 6a shows
the daily maximum PV gradients calculated as a function of EqL, a measure of the strength of the
polar vortex as a transport barrier (e.g., Manney et al., 1994a, 2011; Lawrence et al., 2014). Although
400 the major SSW commenced and the vortex split in early January 2013 (with concurrent reversal of
the high latitude zonal mean winds), PV gradients remained near the climatological average until
the end of January, then dropped rapidly to very low values indicating that the vortex was no longer
well defined. The Zonal mean winds (not shown) began to increase in February when the reforming
vortex was relatively symmetric and pole-centered. The vortex recovered strongly in the middle and
405 upper stratosphere by mid-February, but very weak PV gradients along the edge of the reformed
vortex in the lower stratosphere indicate that it was an insignificant transport barrier there at that
time. The 2010 SSW, in contrast, did not result in a complete breakdown of the lower stratospheric
vortex (previously noted by, e.g., Dörnbrack et al., 2012).

Figure 6b and c show daily time series of SVA (the portion of the vortex that is equatorward of
410 the latitude of polar night), indicating where, combined with low temperatures, there is potential for
chlorine-catalyzed O_3 loss. Figure 6b shows SVA expressed as a fraction of the vortex area. There
were periods in December in both 2010 and 2012 when the vortex received much more sunlight than
usual. In both winters, these periods were associated with very disturbed conditions in which the
vortex was highly elongated and split or nearly split in the lower stratosphere (e.g., Cohen et al., 2010

415 and Wang and Chen, 2010 discuss lower stratospheric vortex disturbances in December 2009); in
December 2010, however, these periods were unusually warm, with no PSC activity (e.g., Dörnbrack
et al., 2012). In addition to those substantial periods in December 2012, most of the vortex (or
more precisely, the offspring vortices following the split) sat in regions that experienced sunlight
throughout January 2013. Figure 6c shows SVA and total vortex area expressed as a percentage of
420 the hemisphere, demonstrating that not only was the sunlit vortex area unusually large in 2012/13,
but the total vortex size was also exceptionally large during December 2012.

Another diagnostic examined is the vortex-temperature concentricity (**VTE**), calculated by deter-
mining the degree to which the centroids of the vortex and cold regions are colocated (Lawrence
et al., 2014). These calculations (not shown) indicate a fairly typical degree of concentricity in much
425 of December 2012 prior to the SSW, but with unusual excursions to very low values in the first ap-
proximately 10 days of December and the first several days of January immediately before the SSW.
Low **VTE** vortex-temperature concentricity is associated with a cold region near the vortex edge that
experiences stronger winds, thus facilitating the processing of more air through regions with PSCs;
previous studies have shown that this results in more extensive chlorine activation (Santee et al.,
430 2003, and references therein).

In the following section we look at the effects of the vortex, temperature, and PSC evolution on
MLS-observed trace gas distributions in the 2012/13 winter.

4 Lower stratospheric trace gas evolution in 2012/13

4.1 Overview and average trace gas evolution

435 Figure 7 shows maps of MLS trace gases on selected days during January 2013. The persistence of
strong N_2O gradients across the vortex edge demonstrates clearly that air in the offspring vortices
remained well confined through January 2013. When the vortices merged at the end of January, PV
gradients weakened, and some mixing was evident (e.g., in the 0 to 45° E sector on 31 January),
but the well-defined region of low N_2O values indicates that most of the air in the reunified vortex
440 remained fairly isolated.

Consistent with the large region of temperatures below T_{NAT} on 1 January, HNO_3 values were
very low through much of the vortex. While vortex HNO_3 did increase slightly after temperatures
rose above the PSC threshold on ~ 5 January, it remained much lower than is typical in warm Arctic
winters in the confined region of each offspring vortex, suggesting that substantial denitrification
445 had occurred. Chlorine was strongly activated on 1 January, and ~~well-confined regions of low HCl~~
persisted persistent well-defined regions of confined low HCl were seen in the offspring vortices
through January. Throughout the period after the vortex split, the offspring vortices were mostly in
regions that receive sunlight, and thus ClO remained elevated within them. Some chlorine activation
was still apparent when the vortices merged at the end of January. The unusually low HNO_3 values

450 may have inhibited reformation of ClONO₂, the typical pathway for rapid chlorine deactivation in the Arctic (Douglass et al., 1995; Santee et al., 2008, and references therein).

On 1 January, ozone values were high through most of the vortex. The values in the offspring vortices decreased throughout January, consistent with chlorine-catalyzed ozone loss in both offspring vortices. It is not obvious from the ozone fields themselves whether the low values inside the merged vortex originated from the offspring vortices or from air drawn in from low latitudes; low N₂O values (characteristic of the vortex) in the same region suggest the former.

Figures 8 and 9 give a more comprehensive view of the trace gas evolution in the 2012/13 winter, showing EqL/time plots of K_{eff} and MLS trace gases at 490 K, and potential temperature/time sections of vortex-averaged (over both offspring vortices) trace gases, respectively. Low K_{eff} values coincident with strong PV gradients (Fig. 8a) confirm that the vortices ~~were well-confined~~ represented a strong transport barrier through January, with a rapidly shrinking isolated region in early February, and complete dissipation of the vortex as a significant transport barrier by late February. The continuing decline of N₂O into early February (Fig. 8b), coupled with strong gradients across the vortex edge, confirms the isolation of the vortex and indicates that descent continued into early February. Low values of and strong gradients in N₂O through late February indicate the persistence of a well-defined vortex region. HNO₃ values also remained low through mid-February in most of the vortex region (Fig. 8c). Low HCl and high ClO values (Fig. 8d and e) were present until early February, when a rapid increase in HCl and decrease in ClO indicates deactivation. The rapid decrease in ozone in late December through January, when K_{eff} , PV gradients (see Fig. 6a and overlaid contours in Fig. 8), and N₂O all indicate that the vortex was still isolated and confined descent continued, implies chemical ozone destruction. Because descent brings down air rich in ozone, the amount of chemical ozone destruction likely exceeded the observed decrease in ozone abundances.

Figure 9a shows a slight transient increase in N₂O below 600 K at the time of the vortex split (~ 8 January), suggesting a small amount of associated mixing. The downward tilt of the contours, however, continues through the time when the offspring vortices begin to merge, after which the upward tilt of N₂O contours at the lowest levels and sharp increase at ~ 500–650 K indicate enhanced mixing.

Low vortex-averaged HNO₃ (Fig. 9b) persisted from about 440 to 580 K through January, after PSCs had evaporated (Fig. 3), with the altitude of the lowest values decreasing gradually ~~through~~ January, from about 530 to 480 K, from late December through mid-January. The episodic higher values near 420 K in late December and early January suggest renitrication as PSC particles fell to levels where there was a much smaller region of $T \leq T_{\text{NAT}}$ (see Fig. 3) and evaporated/sublimated. The persistence of low vortex HNO₃ after temperatures had risen and the evidence of renitrication are similar to the behavior seen in the very cold period before the SSW in late January 2010 (Khosrawi et al., 2011). Figure 10 provides further evidence for the occurrence of denitrication/renitrication: on 16 December, MLS measurements along an orbit track show very low gas-

phase HNO_3 values colocated with a region of CALIPSO PSC observations composed largely of MIX1 and MIX2, with some MIX2E. On 28 December, a region of low HNO_3 remained although no PSCs were observed, and an underlying enhancement of HNO_3 shows the signature of renitrification. An estimate of particle size and number density using the method described by Lambert et al. (2012) indicates the presence of numerous large particles (radii $> 6 \mu\text{m}$) on 16 December. Figure 3 (bottom panel) shows that liquid/NAT mixture PSCs were abundant throughout the cold period in December 2012, implying that the processes exemplified in Fig. 10 were widespread during this period.

The region of activated chlorine (low HCl, high ClO in Fig. 9c and d) extended above 600 K through mid-January. HCl gradually increased at the highest levels shortly after the vortex split; evidence of somewhat more mixing at these levels than at lower levels is apparent in the vortex-averaged N_2O (Fig. 9a). Increasing HCl values extended to lower and lower levels through February. The maxima in ClO around 20 December and from about 5 through 20 January were concurrent with maxima in SVA (Fig. 6). The SVA as a fraction of the vortex reached a maximum of 1.0 after HCl began to rise; consequently, maximum ClO values were observed after deactivation had already begun because more of the active chlorine was converted to ClO even though the absolute amount was decreasing. Note that the partitioning of active chlorine also shifts towards ClO at higher temperatures (e.g., Santee et al., 2010, and references therein), which may have contributed to these variations. The low abundances of HNO_3 may have hindered reformation of ClONO_2 (typically the initial deactivation pathway in the Arctic, e.g., Douglass et al., 1995; Santee et al., 2008) and thus delayed deactivation. ClO dropped to near zero by about 5 February, over a month after PSCs were last observed.

The vortex-averaged ozone time series (Fig. 9e) shows decreasing values at levels between about 450 and 600 K from before mid-December until the vortex split. After the vortex split, increases were seen at the higher levels, but ozone decreased more rapidly between about 450 and 550 K. After the vortices merged, vortex-averaged ozone increased throughout the lower stratosphere, consistent with some mixing during their reunification.

4.2 Trace gas evolution in the offspring vortices

The maps shown above (Fig. 7) indicated clear differences in the dynamical and chemical characteristics of the two offspring vortices in January 2013. Figure 11 shows the detailed evolution of MLS trace gases at 490 K in the individual offspring vortices, in the context of vortex conditions. The Canadian vortex (in dark red) encompassed about 20–40% of the total vortex area (dots on Fig. 11b). As was apparent on individual days in Fig. 7, the Canadian vortex was closer to the pole than the Siberian vortex (in orange) in early January, but moved to near 50°N latitude by mid-January (Fig. 11a), completely equatorward of polar night. The average latitude of the Siberian vor-

tex was near 60° N in early January to over 70° N in late January, with a corresponding late-January decrease in SVA (though 60–80 % of that vortex still experienced sunlight).

Average temperatures in January were considerably lower in the Canadian than in the Siberian vortex (Fig. 11c). Even in the Canadian vortex, however, the minimum temperatures were near or higher than T_{NAT} (the minimum temperatures in Fig. 2 reflect those in the Canadian vortex). N_2O values (Fig. 11d) dropped steadily in both vortices until about 24 January. A small, brief increase at the time of the vortex split suggests transient mixing into the Siberian vortex, and a small increase in N_2O in the Canadian vortex in the last few days before the merge suggests increased mixing into that offspring vortex. On average, N_2O values were similar in the two offspring vortices during the period when they were separated.

The average HNO_3 values seen in Fig. 11e in the Canadian vortex were about 1 ppbv lower than those in the larger Siberian vortex, and usually below any previously observed by Aura MLS in the Arctic in January (see below). Because the vortices experienced sunlight over much of their areas during January, the possibility that photolysis (usually very slow in the vortex in December and January) contributes to the persistence of low HNO_3 values should be considered. The photochemical lifetime of HNO_3 in winter greatly exceeds 30 days for latitudes poleward of 60°N (comparable to the location of the vortex in December) and ranges from ~ 20 to over 30 days at 50° (near the position of the Canadian vortex in late January) (e.g., Austin et al., 1986). Similarly, the photodissociation rates given by Kawa et al. (1992) as a function of solar zenith angle suggest a lifetime against photolysis of 60 days or more for the vortex conditions in January 2013, except for those of the Canadian vortex in late January, when the expected lifetime is near 30 days. Photolysis of HNO_3 may thus have played some role (albeit small) in maintaining low HNO_3 in the Canadian vortex in January 2013. But the primary mechanism leading to lower HNO_3 in the Canadian than in the Siberian vortex is likely to have been the non-uniform distribution of denitrification within the parent vortex arising from the persistent location of the cold region towards that side of the vortex before the split (see Fig. 1 and the Supplement).

The large PSC particle surface area present within the vortex through most of December 2012 (Fig. 4) resulted in strong chlorine activation beginning in early December, seen both in the large drop in HCl and the increase in ClO. As noted above, maxima in ClO correspond closely to periods when most of the vortex area was in sunlight. In particular, the peaks in late December and in the larger Siberian vortex in early January were contemporaneous with increases in SVA for those vortices, and the dramatic increase in ClO in the Canadian vortex after mid-January (about two weeks after the last occurrence of PSCs) corresponds to the time when that vortex moved fully into latitudes that received sunlight. ClO was significantly higher in the Canadian offspring vortex; that HCl was also significantly lower suggests that the difference in activation between the vortices is not entirely accounted for by differing sunlight levels. This is likely partly due to nonuniform activation in the two offspring vortices at the time of the split – the morphology at that time was

similar to that seen on 11 January 2013 in Fig. 7, with the Canadian vortex more completely filled
560 with very low HCl values than the Siberian vortex. HCl began to increase later in the Canadian
than in the Siberian vortex, but increased more rapidly once it began. Since the Canadian vortex
remained outside the area of polar night after mid-January, the decrease in ClO in that vortex arose
entirely from deactivation; that is, none of the observed decline in ClO came about through changes
in chlorine partitioning induced by changes in sunlight exposure. This unequivocal observation of
565 deactivation well before the vernal equinox is unique in the MLS record. Since photolysis of HNO₃
is the primary source of the NO₂ needed for ClONO₂ production (e.g., Kawa et al., 1992; Douglass
et al., 1995; Santee et al., 2008), the depressed HNO₃ abundances in the Canadian vortex may have
inhibited that deactivation pathway. That HCl in the Canadian vortex began to increase concurrently
with the rapid decrease in ClO is consistent with deactivation occurring through HCl formation to
570 a greater degree than is typical in the Arctic, as discussed in more detail below.

Ozone began to decrease steadily by mid-December (Fig. 11h), indicating that it was decreasing
faster via chemical loss than it was being replenished by diabatic descent. The early onset of rapid
chemical ozone loss is consistent with 60–80 % of the vortex being exposed to sunlight in December
and the consequent high ClO values. On average, ozone was distributed fairly uniformly between
575 the two offspring vortices at the time of the split. Ozone decreased slightly faster in the Canadian
vortex in mid to late January, consistent with greater exposure to sunlight and the higher ClO values
in that vortex. The observed ozone decreases from the maximum in mid-December were about 0.6
and 0.8 ppmv in the Siberian and Canadian vortices, respectively.

4.3 Comparison with other Arctic winters

580 To compare the polar processing in 2012/13 with that in the other Arctic winters observed by Aura
MLS, we show the evolution of N₂O, HNO₃, HCl, ClO, and O₃ averaged over the total vortex area
(that is, encompassing all offspring vortices) (Fig. 12). The evolution of N₂O in December 2012 and
January 2013 (Fig. 12a) was very similar to that in the other Arctic winters observed by Aura MLS,
indicating similar patterns of descent in the vortex. That this was the case for approximately a month
585 following the vortex split in 2013 provides additional evidence of how well the offspring vortices
remained isolated. After late January, when the vortices coalesced, N₂O rose to values much higher
than any previously observed at that time of year.

Vortex-averaged HNO₃ (Fig. 12b) in December was among the lowest in the Aura record, with
the abrupt drop in early December indicating the onset of extensive PSC activity. HNO₃ values re-
590 mained unusually low through early February 2013. The overall vortex average values were roughly
comparable to those in January and February in 2010 and 2011, both winters in which substantial
denitrification has been reported (e.g., Khosrawi et al., 2011; Manney et al., 2011; Wohltmann et al.,
2013). In those winters, however, PSCs persisted at that time, so the degree to which the low values
arose from denitrification rather than sequestration in PSCs is difficult to determine.

595 Consistent with the low temperatures and persistently large PSC surface area (Figs. 2–4), extensive
chlorine activation was observed earlier than in any of the other Arctic winters during which Aura
measurements are available, as seen in the large drop in HCl in early December 2012 in Fig. 12c.
The unusually extensive exposure to sunlight near the time of winter solstice resulted in strongly
elevated (~ 0.5 – 0.7 ppbv in the vortex average) ClO much earlier than in any other winter shown
600 here. Activation also began in early December in the 2011/12 winter (Bernhard et al., 2012; WMO,
2014), but HCl values were less extreme (defining the bottom of the envelope in Fig. 12c), and
maximum ClO values in December remained below 0.4 ppbv (not shown). In both 2010 and 2013,
ClO remained well above zero for about a month (slightly longer in 2013) after the SSWs. In 2013,
ClO remained near its maximum value for over two weeks after temperatures rose above T_{NAT} ,
605 while in 2010, ClO began decreasing immediately after the SSW despite temperatures remaining
below T_{NAT} for about two more weeks (Fig. 2).

Examination of ClO for each individual year indicates that the time for ClO to decline to near-
zero values in 2012/13 after reaching its peak (~ 25 – 30 days) was similar to that in 2010/11 and
2009/10, slightly longer than the 15–20 days in the other observed years. (When deactivation begins
610 before the vernal equinox, however, varying sunlight exposure also affects the timing of the ClO
decline.) The time for HCl to reach a maximum from the beginning of a relatively monotonic rise
(~ 30 – 35 days) in 2012/13 was shorter than that in other years observed by Aura MLS (~ 40 –
60 days). Ozone abundances during the period when deactivation was occurring in 2012/13 were
 ~ 2.5 – 2.7 ppmv, about 0.5–0.7 ppmv lower than those in the years when ClO declined most rapidly.
615 Douglass and Kawa (1999) and Santee et al. (2008) have shown cases where low ozone amounts in
the Arctic favored HCl formation. Thus, both low HNO_3 and low O_3 abundances can affect Arctic
chlorine deactivation. A thorough analysis of interannual variability in chlorine partitioning in the
MLS record would require detailed chemical modeling and is beyond the scope of this paper, but
the relatively slow decline in ClO and relatively rapid rise in HCl in the presence of unusually low
620 HNO_3 and O_3 abundances is consistent with previous observations under similar conditions.

The ozone decrease beginning in mid-December 2012 was earlier than that in any other Arctic
winter observed by Aura. By late January 2013, O_3 was about 0.4 ppmv lower than in any of the
nine other winters shown in Fig. 12. The observed ozone decrease of about 0.6 ppmv between mid-
December and early February is about double the amount of previously observed reductions in this
625 interval, which were less than ~ 0.3 ppmv. Since descent was replenishing vortex O_3 during this
period, the chemical loss was larger than the observed decrease. In the following section, we use
~~trajectory methods~~ [the reverse trajectory and Lagrangian trajectory diagnostic methods described in
section 2.3.3](#) with MLS N_2O , HNO_3 , and O_3 to estimate denitrification and chemical loss amounts.

5 Estimates of chemical ozone loss

630 RT-Reverse trajectory (RT, see section 2.3.3) estimates of chemical O_3 loss and denitrification at
490 K in December 2012 and January 2013 are shown in Fig. 13. The N_2O values (Fig. 13a and
b) indicate uncertainties in the transport calculation, and suggest that the descent in the RT calcu-
lations is too strong or mixing too weak, in that the modelled N_2O drops faster than that observed.
After about 20 January, when the vortices are moving back together, and mixing is starting to in-
crease, the RT underestimate of N_2O becomes larger. Transport errors are larger in the Canadian
635 vortex than in the Siberian vortex. The maximum difference between passive RT and MLS ozone
in both the total vortex average and individual offspring vortex averages is about 0.85 ppmv on
26 January (Fig. 13d), with values of about 0.7 ppmv on 20 January, when overall transport errors
as indicated by N_2O are still relatively small. This agrees well with a rough estimate of chemical
ozone loss using MLS N_2O to estimate vortex-averaged descent as per, e.g., Manney et al. (2006)
(not shown) that indicates a maximum of just over 0.7 ppmv vortex averaged ozone loss on about
20 January near 500 K. Similar calculations for other years (not shown) give chemical loss estimates
between 1 December and 20 January ranging from about 0.2 to 0.4 ppmv at 490 K. As was the
case in 2012/13, the calculations also indicate larger-than-typical transport (N_2O) errors in 2005/06,
645 2008/09, and 2011/12, all years with strong January SSWs; this indicates greater difficulty in simu-
lating transport under disturbed conditions. The lack of significant improvement with more frequent
reinitialization (noted in section 2.3.3) suggests that these increasing errors are more closely related
to larger inaccuracies in the 3-D motion fields under disturbed conditions (and possibly limitations
in the MLS data's ability to capture the finer-scale structure that develops under such conditions)
650 than to trajectory errors accumulated over the duration of the longer runs. Similar patterns of and
interannual variability in estimated ozone loss are found at 460 and 520 K; for 2012/13, the RT
calculations indicate ~ 0.6 ppmv (~ 0.7 ppmv) ozone loss at 460 K (520 K). Transport errors be-
come larger at 550 K, but many years show significant ozone loss (ranging from 0.3 to 0.7 ppmv)
by 20–30 January. About 0.7 ppmv ozone loss was estimated at 550 K in 2012/13.

655 The RT method was also used to estimate the chemical and microphysical processes affecting
 HNO_3 (Fig. 13e and f). In the absence of PSC formation, denitrification, and photolysis, the RT
model predicts a slight increase in vortex HNO_3 from 8 December through January. Instead, ob-
served HNO_3 drops dramatically. This is consistent with sequestration in PSCs during the period
before about 20 December, when observations show large oscillations over a few days that are cor-
related with temperature changes. After a further rapid drop starting about 21 December, HNO_3
660 values remained low through January. Examination of maps of the RT/observed HNO_3 differences
(not shown) indicate that the depression in observed with respect to passively transported HNO_3
was uniformly distributed throughout the vortex during January. These results are consistent with
vortex-averaged denitrification of about 4 ppbv. Examination of a run initialized on 1 January (not
shown) indicates good agreement between RT and MLS HNO_3 throughout the month, with little
665 change in either, confirming that photolysis did not significantly affect vortex HNO_3 .

Livesey et al. (2015) estimated chemical ozone loss during January through March for the 2004/05 through 2012/13 Arctic winters using the MLS Match technique (see also Sect. 2.3.3). We use similar calculations for the December/January period to compare early winter chemical ozone loss in 670 2012/13 with that in previous years observed by Aura MLS (Fig. 14). The values for 2012/13 using this Match method are somewhat smaller than those from the RT and vortex-averaged descent estimates described above, and Livesey et al. (2015) show that their winter-long estimates tend to be in the lower part of the range of values obtained using several other methods and datasets. Uncertainties in Arctic ozone loss estimates are consistently large (e.g., Brakebusch et al., 2013; Livesey et al., 675 2015), but interannual differences in estimates derived from each dataset/method tend to agree well (e.g., Manney et al., 2011), indicating that comparisons of relative values calculated using the same method across the years are robust. The calculations for 1 December through 20 January (Fig. 14, left panel) indicate about twice as much chemical loss near 500 K in 2012/13 as the largest in the previous years. In addition, significant chemical loss before 20 January extended down to 450 K in 680 2012/13, but not in any of the previous winters observed by Aura MLS. The previous years with largest ozone loss at 500 K prior to 20 January were 2005/06 and 2008/09, both years with strong prolonged SSWs in late January. This is consistent with the disturbed vortex prior to these SSWs experiencing more sunlight than is typical.

By 31 January (Fig. 14, right panel), the MLS Match calculations show chemical loss commencing in most of the years studied. In 2012/13, the estimates decrease slightly, and the uncertainties 685 increase, between 20 and 30 January, consistent with the results of the RT calculations that showed increasing errors in transport during that period. The large values in 2009/10 are consistent with the disturbed but very cold vortex in mid-January 2010. In most years, significant early winter ozone loss does not extend down to 450 K even by 31 January. Only 2011/12 shows significant ozone loss 690 at 450 K between 20 and 31 January (but not before 20 January). As noted above, there was also a prolonged SSW in 2011/12 (though that event had a less dramatic and abrupt effect on the lower stratospheric circulation), and some similarities are seen in trace gas evolution.

The results from these chemical ozone loss estimates show that disturbances to the lower stratospheric vortex prior to strong SSWs can be an important factor in controlling early winter ozone 695 loss, largely because they result in significantly greater exposure of the vortex to sunlight during the interval before chlorine is deactivated. In 2012/13, the period with a highly disturbed vortex containing significant amounts of active chlorine persisted for approximately a month after the SSW and consequent increase of temperatures above T_{NAT} , facilitating exceptional early winter chemical ozone loss.

700 6 Conclusions

We have described the evolution of meteorological conditions, polar stratospheric clouds (PSCs), and trace gases in the 2012/13 Arctic winter. Our results give a detailed view of the processes, associated with ~~the vortex split SSW~~ an SSW that split the vortex in early January 2013, that led to more chemical ozone loss in December 2012 and January 2013 than previously observed during that
705 period in the Arctic. Figure 15 provides a schematic of the processes leading to this unusual early winter ozone loss.

Temperature and vortex information from the MERRA and ~~G591~~ GEOS-5.9.1 data assimilation system fields, and PSC information from CALIPSO, show that:

- 710 – The lower stratosphere was unusually cold in December 2012, with a period of ~ 3 weeks with temperatures below the frost point.
- While temperatures on a given date at a given level did not in general set records, they were more consistently low over a deeper layer than usual in December 2012, resulting in greater potential for chlorine activation and ozone loss than in other winters with comparably early SSWs.
- 715 – During the cold period in December 2012, the total PSC particle surface area within the vortex was larger than that in any of the other seven winters observed by CALIPSO.
- The PSCs present during the cold period in December 2012 included a substantial fraction of NAT mixtures with large particles that can sediment quickly.
- Temperatures rose abruptly above the chlorine activation threshold throughout the lower
720 stratosphere a few days before the 6 January onset of the major SSW and the ~ 8 January vortex split.
- The two offspring vortices remained separate, strong (i.e., effective transport barriers), ~~well-confined~~, and largely in regions receiving sunlight until they merged at the end of January.
- 725 – After the vortex split, temperatures in the smaller (20–40% of total vortex area) “Canadian” vortex were significantly lower than those in the larger “Siberian” vortex, though both remained entirely above T_{NAT} .
- After the offspring vortices merged at the end of January, the reunited vortex weakened and enhanced mixing occurred; by mid-February, the vortex ~~became ill-defined~~ no longer represented
730 a significant transport barrier.
- The Canadian vortex was entirely outside of polar night after mid-January, with an average latitude of 50–60° N.

The peculiar meteorological conditions and PSC evolution detailed above gave rise to the following responses in the MLS trace gases:

- 735 – N₂O observations indicate that confined descent in the offspring vortices continued until they merged in late January.
- After a period of about three weeks in December with a large area of PSC mixtures containing solid NAT particles, vortex HNO₃ remained very low through early February, indicating denitrification.
- 740 – HNO₃ was significantly lower (by about 1 ppbv) in the Canadian than in the Siberian vortex, largely as a result of more persistent PSC activity in that portion of the parent vortex before the split.
- HCl and ClO indicate earlier chlorine activation than previously observed by Aura MLS in the Arctic.
- 745 – Peaks in ClO were concurrent with periods when most of the vortex was exposed to sunlight. From mid through late January, ClO was significantly higher (by ~ 0.4 ppbv) in the Canadian than in the Siberian vortex as a result of greater sunlight exposure.
- Chlorine deactivation in January began later in the Canadian than in the Siberian vortex, likely resulting from lower HNO₃ abundances reducing deactivation into ClONO₂.
- 750 – The observed ozone values and decrease from mid-December to early February were unprecedented, with about 0.4 ppmv less ozone in late January 2013 than in any other winter in the [2004/05–2014/15](#) MLS record.

It was thus a unique combination of dynamical processes – that is, persistently low temperatures and a disturbed vortex in December 2012, and the split into two vortices that individually remained
755 isolated through January – that led to the unusual chemical processing and ozone loss (illustrated in Fig. 15).

Estimates of chemical ozone loss using passive subtraction and vortex-averaged descent methods indicate ~ 0.7–0.8 ppmv maximum vortex-averaged chemical loss near 500 K. Passive subtraction calculations also indicate vortex-wide denitrification, resulting in a deficit of about 4 ppbv in vortex-
760 averaged HNO₃ through January.

While quantitative uncertainties in early winter ozone loss estimates are large, calculations using a single method and dataset have been shown to give a robust picture of interannual variability. Comparisons of calculations using a Match method for each winter observed by Aura MLS show that chemical loss in December 2012 and January 2013 was larger than that in any of the other years
765 in that record. While some of those years had significant loss during that period near 500 K, only in 2012/13 was that early winter ozone loss large down through 450 K.

Significant ozone loss before late January was previously seen only in 2005/06 and 2008/09, winters with strong SSWs in January. This emphasizes the importance of disturbances of the lower stratospheric vortex prior to SSWs in the development of conditions promoting chemical ozone
770 destruction in early winter. In particular, disturbed vortices prior to SSWs tend to experience more sunlight than those in overall colder, more quiescent winters, allowing substantial ozone destruction in those cases where temperatures are also persistently low enough for extensive chlorine activation.

The combination of dynamical conditions that led to exceptional chemical ozone loss in December 2012 and January 2013 is, so far, unique in the record of Arctic winter variability. The extensive
775 suite of measurements pertinent to lower stratospheric polar processing available from MLS and CALIPSO for the past decade allowed detailed diagnosis of the processes leading to the unusual early winter ozone loss in 2012/13. Just two years earlier, Arctic winter conditions combined to produce unprecedented springtime ozone loss, arguably resulting in the first “Arctic ozone hole”. The occurrence in two recent winters of vastly different permutations in lower stratospheric meteorology,
780 each unlike any previously observed, and the impact of those dynamical conditions on polar winter chemical processes, argues for the importance of continuing comprehensive composition measurements to enable diagnosis of future extreme variations in polar processing and Arctic ozone loss.

**The Supplement related to this article is available online at
doi:10.5194/acp-0-1-2015-supplement.**

785 *Acknowledgements.* Thanks to the MLS team at JPL (especially Brian Knosp, Ryan Fuller, and William Daffer) for data processing, management and analysis support, and to Ken Minschwaner, Joan Alexander, and Sharon Sessions and her “Research and Communications” class at NMT for helpful comments/discussions; [thanks to the two anonymous referees for their helpful comments](#). Thanks to Steven Pawson and the GMAO for their work in production/distribution of MERRA and GEOS-5.9.1 data. Work at the Jet Propulsion Laboratory, California
790 Institute of Technology, was done under contract with the National Aeronautics and Space Administration.

References

- [Achtert, P. and Tesche, M.: Assessing lidar-based classification schemes for polar stratospheric clouds based on 16 years of measurements at Esrange, Sweden., *J. Geophys. Res.*, 119, 1386–1405, 2014.](#)
- 795 Allen, D. R. and Nakamura, N.: A seasonal climatology of effective diffusivity in the stratosphere, *J. Geophys. Res.*, 106, 7917–7935, 2001.
- [Arnone, E., Castelli, E., Papandrea, E., Carlotti, M., and Dinelli, B. M.: Extreme ozone depletion in the 2010–2011 Arctic winter stratosphere as observed by MIPAS/ENVISAT using a 2-D tomographic approach, *Atmos. Chem. Phys.*, 12, 9149–9165, 2012.](#)
- 800 Austin, J., Garcia, R. R., Russell III, J. M., Solomon, S., and Tuck, A. F.: On the atmospheric photochemistry of nitric acid, *J. Geophys. Res.*, 91, 5477–5485, 1986.
- Bernhard, G., Manney, G., Fioletov, V., Grooß, J.-U., Heikkilä, A., Johnsen, B., Koskela, T., Lakkala, K., Müller, R., Lund Myhre, C., and Rex, M.: Ozone and UV Radiation [In Arctic Report Card 2012], available at: <http://www.arctic.noaa.gov/reportcard> (last access: 13 February 2015), 2012.
- Bloom, S. C., Takacs, L. L., da Silva, A. M., and Ledvina, D.: Data assimilation using incremental analysis 805 updates, *Mon. Weather Rev.*, 124, 1256–1271, 1996.
- Brakebusch, M., Randall, C. E., Kinnison, D. E., Tilmes, S., Santee, M. L., and Manney, G. L.: Evaluation of whole atmosphere community climate model simulations of ozone during Arctic winter 2004–2005, *J. Geophys. Res.*, 118, 2673–2688, doi:10.1002/jgrd.50226, 2013.
- Butchart, N. and Remsberg, E. E.: The area of the stratospheric polar vortex as a diagnostic for tracer transport 810 on an isentropic surface, *J. Atmos. Sci.*, 43, 1319–1339, 1986.
- Charlton, A. J. and Polvani, L. M.: A new look at stratospheric sudden warmings. Part I: Climatology and modeling benchmarks, *J. Climate*, 20, 449–469, 2007.
- Charlton-Perez, A. J., Polvani, L. M., Austin, J., and Li, F.: The frequency and dynamics of stratospheric sudden warmings in the 21st century, *J. Geophys. Res.*, 113, D16116, doi:10.1029/2007JD009571, 2008.
- 815 Cohen, J., Foster, J., Barlow, M., Saito, K., and Jones, J.: Winter 2009–2010: a case study of an extreme Arctic oscillation event, *Geophys. Res. Lett.*, 37, L17707, doi:10.1029/2010GL044256, 2010.
- Coy, L. and Pawson, S.: The major stratospheric sudden warming of January 2013: analyses and forecasts in the GEOS-5 data assimilation system, *Mon. Weather Rev.*, 143, 491–510, 2015.
- Dörnbrack, A., Pitts, M. C., Poole, L. R., Orsolini, Y. J., Nishii, K., and Nakamura, H.: The 2009–2010 Arctic 820 stratospheric winter – general evolution, mountain waves and predictability of an operational weather forecast model, *Atmos. Chem. Phys.*, 12, 3659–3675, doi:10.5194/acp-12-3659-2012, 2012.
- Douglass, A. and Kawa, S.: Contrast between 1992 and 1997 high-latitude spring halogen occultation experiment observations of lower stratospheric HCl, *J. Geophys. Res.*, 104, 18739–18754, 1999.
- Douglass, A. R., Schoeberl, M. R., Stolarski, R. S., Waters, J. W., III, J. M. R., Roche, A. E., and Massie, S. T.: 825 Interhemispheric differences in springtime production of HCl and ClONO₂ in the polar vortices, *J. Geophys. Res.*, 100, 13967–13978, 1995.
- Drdla, K. and Müller, R.: Temperature thresholds for chlorine activation and ozone loss in the polar stratosphere, *Ann. Geophys.*, 30, 1055–1073, doi:10.5194/angeo-30-1055-2012, 2012.
- Dunkerton, T. J. and Delisi, D. P.: Evolution of potential vorticity in the winter stratosphere of January–February 830 1979, *J. Geophys. Res.*, 91, 1199–1208, 1986.

- Fueglistaler, S., Buss, S., Luo, B. P., Wernli, H., Flentje, H., Hostetler, C. A., Poole, L. R., Carslaw, K. S., and Peter, Th.: Detailed modeling of mountain wave PSCs, *Atmos. Chem. Phys.*, 3, 697–712, doi:10.5194/acp-3-697-2003, 2003.
- Gobbi, G. P.: Lidar estimation of stratospheric aerosol properties: Surface, volume, and extinction to backscatter ratio, *J. Geophys. Res.*, 100, 11219–11235, 1995.
- 835 Goncharenko, L., Chau, J. L., Condor, P., Coster, A., and Benkevitch, L.: Ionospheric effects of sudden stratospheric warming during moderate-to-high solar activity: case study of January 2013, *Geophys. Res. Lett.*, 40, 4982–4986, doi:10.1002/grl.50980, 2013.
- Hanson, D. and Mauersberger, K.: Laboratory studies of the nitric acid trihydrate: implications for the south polar stratosphere, *Geophys. Res. Lett.*, 15, 855–858, 1988.
- 840 Haynes, P. and Shuckburgh, E.: Effective diffusivity as a diagnostic of atmospheric transport 1. Stratosphere, *J. Geophys. Res.*, 105, 22777–22794, 2000.
- Hitchcock, P. and Shepherd, T. G.: Zonal-mean dynamics of extended recoveries from stratospheric sudden warmings, *J. Atmos. Sci.*, 70, 688–707, 2013.
- 845 Hitchcock, P., Shepherd, T. G., and Manney, G. L.: Statistical characterization of Arctic polar-night jet oscillation events, *J. Climate*, 26, 2096–2116, 2013.
- [Hommel, R., Eichmann, K.-U., Aschmann, J., Bramstedt, K., Weber, M., von Savigny, C., Richter, A., Rozanov, A., Wittrock, F., Khosrawi, F., Bauer, R., and Burrows, J. P.: Chemical ozone loss and ozone mini-hole event during the Arctic winter 2010/2011 as observed by SCIAMACHY and GOME-2, *Atmos. Chem. Phys.*, 14, 3247–3276, 2014.](#)
- 850 Hostetler, C. A., Liu, Z., Reagan, J., Vaughan, M., Winker, D., Osborn, M., Hunt, W. H., Powell, K. A., and Trepte, C.: CALIOP Algorithm Theoretical Basis Document: Calibration and Level 1 Products, Tech. Rep., NASA Langley Research Center, location is Hampton, VA USA, PC-SCI-201, NASA Langley Research Center, available at: <http://www-calipso.larc.nasa.gov/resources/pdfs/PC-SCI-201v1.0.pdf> (last access: 13 February 2015), 2006.
- 855 Hunt, W. H., Winker, D. M., Vaughan, M. A., Powell, K. A., Lucker, P. L., and Weimer, C.: CALIPSO lidar description and performance assessment, *J. Atmos. Ocean. Tech.*, 26, 1214–1228, 2009.
- Kawa, S. R., Fahey, D. W., Heidt, L. E., Pollock, W. H., Solomon, S., Anderson, D. E., Loewenstein, M., Proffitt, M. H., Margitan, J. J., and Chan, K. R.: Photochemical partitioning of the reactive nitrogen and chlorine reservoirs in the high-latitude stratosphere, *J. Geophys. Res.*, 97, 7905–7923, 1992.
- 860 Khosrawi, F., Urban, J., Pitts, M. C., Voelger, P., Achtert, P., Kaphlanov, M., Santee, M. L., Manney, G. L., Murtagh, D., and Fricke, K.-H.: Denitrification and polar stratospheric cloud formation during the Arctic winter 2009/2010, *Atmos. Chem. Phys.*, 11, 8471–8487, doi:10.5194/acp-11-8471-2011, 2011.
- Kuttippurath, J. and Nikulin, G.: A comparative study of the major sudden stratospheric warmings in the Arctic winters 2003/2004–2009/2010, *Atmos. Chem. Phys.*, 12, 8115–8129, doi:10.5194/acp-12-8115-2012, 2012.
- 865 Kuttippurath, J., Godin-Beekmann, S., Lefèvre, F., and Goutail, F.: Spatial, temporal, and vertical variability of polar stratospheric ozone loss in the Arctic winters 2004/2005–2009/2010, *Atmos. Chem. Phys.*, 10, 9915–9930, doi:10.5194/acp-10-9915-2010, 2010.

- [Kuttippurath, J., Godin-Beekmann, S., Lefèvre, F., Nikulin, G., Santee, M. L., and Froidevaux, L.: Record-breaking ozone loss in the Arctic winter 2010/2011: comparison with 1996/1997, *Atmos. Chem. Phys.*, **12**, 7073–7085, 2012.](#)
- Lambert, A., Santee, M. L., Wu, D. L., and Chae, J. H.: A-train CALIOP and MLS observations of early winter Antarctic polar stratospheric clouds and nitric acid in 2008, *Atmos. Chem. Phys.*, **12**, 2899–2931, doi:10.5194/acp-12-2899-2012, 2012.
- 875 ~~Lawrence, Z. D. and Manney, G. L.: [On the characterization of split vortices](#)~~ [Characterizing stratospheric polar vortices with algorithms for image processing and feature tracking](#), in preparation, 2015.
- Lawrence, Z. D., Manney, G. L., Minschwaner, K., Santee, M. L., and Lambert, A.: Comparisons of polar processing diagnostics from 34 years of the ERA-Interim and MERRA reanalyses, *Atmos. Chem. Phys. Discuss.*, **14**, 31361–31408, doi: 2014-15, 3873–3892, 2015.
- 880 Limbach, S., Schömer, E., and Wernli, H.: Detection, tracking and event localization of jet stream features in 4-D atmospheric data, *Geosci. Model Dev.*, **5**, 457–470, doi:10.5194/gmd-5-457-2012, 2012.
- Livesey, N. J.: Aura Microwave Limb Sounder Lagrangian Trajectory Diagnostics Users’ guide and file description document, Tech. rep., Jet Propulsion Laboratory, location is Pasadena, CA USA, available at: <http://mls.jpl.nasa.gov/data/ltd.php> (last access: 13 February 2015), 2013.
- 885 Livesey, N. J., Read, W. G., Froidevaux, L., Lambert, A., Manney, G. L., Pumphrey, H. C., Santee, M. L., Schwartz, M. J., Wang, S., Cofield, R. E., Cuddy, D. T., Fuller, R. A., Jarnot, R. F., Jiang, J. H., Knosp, B. W., Stek, P. C., Wagner, P. A., and Wu, D. L.: EOS MLS Version 3.3 / 3.4 Level 2 data quality and description document, Tech. rep., Jet Propulsion Laboratory, location is Pasadena, CA USA, available at: <http://mls.jpl.nasa.gov/> (last access: 13 February 2015), 2013.
- 890 Livesey, N. J., Santee, M. L., and Manney, G. L.: A Match-based approach to the estimation of polar stratospheric ozone loss using Aura Microwave Limb Sounder observations, ~~submitted to *Atmos. Chem. Phys.*~~, [Atmos. Chem. Phys. Disc.](#), **15**, 10,041–10,083, 2015.
- Manney, G. L., Zurek, R. W., Gelman, M. E., Miller, A. J., and Nagatani, R.: The anomalous Arctic lower stratospheric polar vortex of 1992–1993, *Geophys. Res. Lett.*, **21**, 2405–2408, 1994a.
- 895 Manney, G. L., Zurek, R. W., O’Neill, A., and Swinbank, R.: On the motion of air through the stratospheric polar vortex, *J. Atmos. Sci.*, **51**, 2973–2994, 1994b.
- Manney, G. L., Zurek, R. W., Froidevaux, L., Waters, J. W., O’Neill, A., and Swinbank, R.: Lagrangian transport calculations using UARS data. Part II: Ozone, *J. Atmos. Sci.*, **52**, 3069–3081, 1995a.
- Manney, G. L., Zurek, R. W., Lahoz, W. A., Harwood, R. S., Gille, J. C., Kumer, J. B., Mergenthaler, J. L.,
900 Roche, A. E., O’Neill, A., Swinbank, R., and Waters, J. W.: Lagrangian Transport Calculations Using UARS Data. Part I. Passive Tracers., *J. Atmos. Sci.*, **52**, 3049–3068, 1995b.
- Manney, G. L., Lahoz, W. A., Swinbank, R., O’Neill, A., Connew, P. M., and Zurek, R. W.: Simulation of the December 1998 stratospheric major warming, *Geophys. Res. Lett.*, **26**, 2733–2736, 1999a.
- Manney, G. L., Michelsen, H. A., Santee, M. L., Gunson, M. R., Irion, F. W., Roche, A. E., and Livesey, N. J.:
905 Polar vortex dynamics during spring and fall diagnosed using trace gas observations from the Atmospheric Trace Molecule Spectroscopy instrument, *J. Geophys. Res.*, **104**, 18841–18866, 1999b.

- Manney, G. L., Froidevaux, L., Santee, M. L., Livesey, N. J., Sabutis, J. L., and Waters, J. W.: Variability of ozone loss during Arctic winter (1991 to 2000) estimated from UARS Microwave Limb Sounder measurements, *J. Geophys. Res.*, 108, 4149, doi:10.1029/2002JD002634, 2003.
- 910 Manney, G. L., Krüger, K., Sabutis, J. L., Sena, S. A., and Pawson, S.: The remarkable 2003–2004 winter and other recent warm winters in the Arctic stratosphere since the late 1990s, *J. Geophys. Res.*, 110, D04107, doi:10.1029/2004JD005367, 2005.
- Manney, G. L., Santee, M. L., Froidevaux, L., Hoppel, K., Livesey, N. J., and Waters, J. W.: EOS MLS observations of ozone loss in the 2004–2005 Arctic winter, *Geophys. Res. Lett.*, 33, L04802, 915 doi:10.1029/2005GL024494, 2006.
- Manney, G. L., Daffer, W. H., Zawodny, J. M., Bernath, P. F., Hoppel, K. W., Walker, K. A., Knosp, B. W., Boone, C., Remsberg, E. E., Santee, M. L., Harvey, V. L., Pawson, S., Jackson, D. R., Deaver, L., McElroy, C. T., McLinden, C. A., Drummond, J. R., Pumphrey, H. C., Lambert, A., Schwartz, M. J., Froidevaux, L., McLeod, S., Takacs, L. L., Suarez, M. J., Trepte, C. R., Cuddy, D. C., Livesey, N. J., Harwood, R. S., and 920 Waters, J. W.: Solar occultation satellite data and derived meteorological products: sampling issues and comparisons with Aura Microwave Limb Sounder, *J. Geophys. Res.*, 112, D24S50, doi:10.1029/2007JD008709, 2007.
- Manney, G. L., Santee, M. L., Rex, M., Livesey, N. J., Pitts, M. C., Veefkind, P., Nash, E. R., Wohltmann, I., Lehmann, R., Froidevaux, L., Poole, L. R., Schoeberl, M. R., Haffner, D. P., Davies, J., Dorokhov, V., Ger- 925 nandt, H., Johnson, B., Kivi, R., Kyrö, E., Larsen, N., Levelt, P. F., Makshtas, A., McElroy, C. T., Nakajima, H., Parrondo, M. C., Tarasick, D. W., von der Gathen, P., Walker, K. A., and Zinoviev, N. S.: Unprecedented Arctic ozone loss in 2011, *Nature*, 478, 469–475, 2011.
- Matthewman, N. J., Esler, J. G., Charlton-Perez, A. J., and Polvani, L. M.: A New look at stratospheric sudden warmings. Part III: Polar vortex evolution and vertical structure, *J. Climate*, 22, 1566–1585, 2009.
- 930 Mitchell, D. M., Charlton-Perez, A. J., and Gray, L. J.: Characterizing the Variability and Extremes of the stratospheric polar vortices using 2D moment analysis, *J. Atmos. Sci.*, 68, 1194–1213, 2011.
- [Molod, A., Takacs, L., Suarez, M., and Bacmeister, J.: Development of the GEOS-5 Atmospheric General Circulation Model: Evolution from MERRA to MERRA2, *Geosci. Model Dev. Disc.*, 7, 7575–7617, 2014.](#)
- [Morris, G. A., Schoeberl, M. R., Sparling, L. C., Newman, P. A., Lait, L. R., Elson, L., Waters, J., Suttie, R. A., Roche, A., Kumer, J., and Russell III, J. M.: Trajectory mapping and applications to data from the Upper 935 Atmosphere Research Satellite, *J. Geophys. Res.*, 100, 16,491–16,505, 1995.](#)
- Nakamura, N.: Two-dimensional mixing, edge formation, and permeability diagnosed in area coordinates, *J. Atmos. Sci.*, 53, 1524–1537, 1996.
- Naujokat, B., Krüger, K., Matthes, K., Hoffmann, J., Kunze, M., and Labitzke, K.: The early major warming in 940 December 2001 – exceptional?, *Geophys. Res. Lett.*, 29, 2023, doi:10.1029/2002GL015316, 2002.
- Pitts, M. C., Poole, L. R., and Thomason, L. W.: CALIPSO polar stratospheric cloud observations: second-generation detection algorithm and composition discrimination, *Atmos. Chem. Phys.*, 9, 7577–7589, doi:10.5194/acp-9-7577-2009, 2009.
- Pitts, M. C., Poole, L. R., Dörnbrack, A., and Thomason, L. W.: The 2009–2010 Arctic polar stratospheric 945 cloud season: a CALIPSO perspective, *Atmos. Chem. Phys.*, 11, 2161–2177, doi:10.5194/acp-11-2161-2011, 2011.

- Pitts, M. C., Poole, L. R., Lambert, A., and Thomason, L. W.: An assessment of CALIOP polar stratospheric cloud composition classification, *Atmos. Chem. Phys.*, 13, 2975–2988, doi:10.5194/acp-13-2975-2013, 2013.
- 950 Randel, W. J. and Boville, B. A.: Observations of a major stratospheric warming during December 1984, *J. Atmos. Sci.*, 44, 2179–2186, 1987.
- Rex, M., von der Gathen, P., Harris, N. R. P., Lucic, D., Knudsen, B. M., Braathen, G. O., Reid, S. J., De Backer, H., Claude, H., Fabian, R., Fast, H., Gil, M., Kyrö, E., Mikkelsen, I. S., Rummukainen, M., Smit, H. G., Stähelin, J., Varotsos, C., and Zaitcev, I.: In-situ measurements of stratospheric ozone depletion rates in
955 the Arctic winter 1991/1992: A Lagrangian approach, *J. Geophys. Res.*, 103, 5843–5853, 1998.
- Rex, M., von der Gathen, P., Braathen, G. O., Harris, N. R. P., Reimer, E., Beck, A., Alfier, R., Krüger-Carstensen, R., Chipperfield, M., De Backer, H., Balis, D., O’Connor, F., Dier, H., Dorokhov, V., Fast, H., Gamma, A., Gil, M., Kyrö, E., Litynska, Z., Mikkelsen, I. S., Molyneux, M., Murphy, G., Reid, S. J., Rummukainen, M., and Zerefos, C.: Chemical Ozone Loss in the Arctic Winter 1994/1995 as Determined by the
960 Match Technique, *J. Atmos. Chem.*, 32, 35–39, 1999.
- Rex, M., Salawitch, R. J., Harris, N. R. P., von der Gathen, P., Braathen, G. O., Schulz, A., Deckelmann, H., Chipperfield, M., Sinnhuber, B.-M., Reimer, E., Alfier, R., Bevilacqua, R., Hoppel, K., Fromm, M., Lumpe, J., Küllmann, H., Kleinböhl, A., Bremer, H., von König, M., Künzi, K., Toohey, D., Vömel, H., Richard, E., Aikin, K., Jost, H., Greenblatt, J. B., Loewenstein, M., Podolske, J. R., Webster, C. R., Flesch, G. J., Scott,
965 D. C., Herman, R. L., Elkins, J. W., Ray, E. A., Moore, F. L., Hurst, D. F., Romashkin, P., Toon, G. C., Sen, B., Margitan, J. J., Wennberg, P., Neuber, R., Allart, M., Bojkov, B. R., Claude, H., Davies, J., Davies, W., De Backer, H., Dier, H., Dorokhov, V., Fast, H., Kondo, Y., Kyrö, E., Litynska, Z., Mikkelsen, I. S., Molyneux, M. J., Moran, E., Nagai, T., Nakane, H., Parrondo, C., Ravagnani, F., Skrivankova, P., Viatte, P., and Yushkov, V.: Chemical depletion of Arctic ozone in winter 1999/2000, *J. Geophys. Res.*, 107, 8276,
970 doi:10.1029/2001JD000533, 2002.
- Rex, M., Salawitch, R. J., Santee, M. L., Waters, J. W., Hoppel, K., and Bevilacqua, R.: On the unexplained stratospheric ozone losses during cold Arctic Januaries, *Geophys. Res. Lett.*, 30, 1008, doi:10.1029/2002GL016008, 2003.
- Rienecker, M. M., Suarez, M. J., Todling, R., Bacmeister, J., Takacs, L., Liu, H.-C., Gu, W., Sienkiewicz, M.,
975 Koster, R. D., Gelaro, R., Stajner, I., and Nielsen, E.: The GEOS-5 Data Assimilation System – Documentation of versions 5.0.1, 5.1.0, and 5.2.0, Tech. Rep., TM-2008-104606, NASA, Goddard Space Flight Center, Greenbelt, MD USA, 2008.
- Rienecker, M. M., Suarez, M. J., Gelaro, R., Todling, R., Bacmeister, J., Liu, E., Bosilovich, M. G., Schubert, S. D., Takacs, L., Kim, G.-K., Bloom, S., Chen, J., Collins, D., Conaty, A., Da Silva, A., Gu, W., Joiner, J.,
980 Koster, R. D., Lucchesi, R., Molod, A., Owens, T., Pawson, S., Pegion, P., Redder, C. R., Reichle, R., Robertson, F. R., Ruddick, A. G., Sienkiewicz, M., and Woollen, J.: MERRA: NASA’s modern-era retrospective analysis for research and applications, *J. Climate*, 24, 3624–3648, 2011.
- Santee, M. L., Manney, G. L., Waters, J. W., and Livesey, N. J.: Variations and climatology of ClO in the polar lower stratosphere from UARS microwave limb sounder measurements, *J. Geophys. Res.*, 108, 4454,
985 doi:10.1029/2002JD003335, 2003.

- Santee, M. L., MacKenzie, I. A., Manney, G. L., Chipperfield, M. P., Bernath, P. F., Walker, K. A., Boone, C. D., Froidevaux, L., Livesey, N. J., and Waters, J. W.: A study of stratospheric chlorine partitioning based on new satellite measurements and modeling, *J. Geophys. Res.*, 113, D12307, doi:10.1029/2007JD009057, 2008.
- 990 Santee, M. L., Sander, S. P., Livesey, N. J., and Froidevaux, L.: Constraining the chlorine monoxide (ClO)/chlorine peroxide (ClOOCl) equilibrium constant from Aura microwave limb sounder measurements of nighttime ClO, *P. Natl. Acad. Sci. USA*, 107, 6588–6593, 2010.
- Schoeberl, M. R., Lait, L. R., Newman, P. A., and Rosenfield, J. E.: The structure of the polar vortex, *J. Geophys. Res.*, 97, 7859–7882, 1992.
- 995 Singleton, C. S., Randall, C. E., Chipperfield, M. P., Davies, S., Feng, W., Bevilacqua, R. M., Hoppel, K. W., Fromm, M. D., Manney, G. L., and Harvey, V. L.: 2002-2003 Arctic ozone loss deduced from POAM III satellite observations and the SLIMCAT chemical transport model, *Atmos. Chem. Phys.*, 5, 597–609, doi:10.5194/acp-5-597-2005, 2005.
- [Sinnhuber, B.-M., Stiller, G., Ruhnke, R., von Clarmann, T., Kellmann, S., and Aschmann, J.: Arctic winter](#)
1000 [2010/2011 at the brink of an ozone hole, *Geophys. Res. Lett.*, L24814, doi:10.1029/2011GL049784, 2011.](#)
- Solomon, S.: Stratospheric ozone depletion: a review of concepts and history, *Rev. Geophys.*, 37, 275–316, 1999.
- von der Gathen, P., Rex, M., Harris, N. R., Lucic, D., Knudsen, B. M., Braathen, G. O., De, H., Fabian, R., Fast, H., Gil, M., Kyrö, E., Mikkelsen, I. S., Rummukainen, M., Stähelin, J., and Varotsos, C.: Observational
1005 evidence for chemical ozone depletion over the Arctic in winter 1991–92, *Nature*, 375, 131–134, 1995.
- Wang, L. and Chen, W.: Downward Arctic Oscillation signal associated with moderate weak stratospheric polar vortex and the cold December 2009, *Geophys. Res. Lett.*, 37, L09707, doi:10.1029/2010GL042659, 2010.
- Waters, J.W., Froidevaux, L., Harwood, R. S., Jarnot, R. F., Pickett, H. M., Read, W. G., Siegel, P. H., Cofield, R. E., Filipiak, M. J., Flower, D. A., Holden, J. R., Lau, G. K., Livesey, N. J., Manney, G. L., Pumphrey, H.
1010 C., Santee, M. L., Wu, D. L., Cuddy, D. T., Lay, R. R., Loo, M. S., Perun., V. S., Schwartz, M. J., Stek, P. C., Thurstans, R. P., Chandra, K. M., Chavez, M. C., Chen, G., Boyles, M. A., Chudasama, B. V., Dodge, R., Fuller, R. A., Girard, M. A., Jiang, J. H., Jiang, Y., Knosp, B. W., LaBelle, R. C., Lam, J. C., Lee, K. A., Miller, D., Oswald, J. E., Patel, N. C., Pukala, D. M., Quintero, O., Scaff, D. M., Snyder, W. V., Tope, M. C., Wagner, P. A., and Walch, M. J.: The Earth Observing System Microwave Limb Sounder (EOS MLS) on
1015 the Aura satellite, *IEEE Trans. Geosci. Remote Sens.*, 44, 1075–1092, 2006.
- Wegner, T., Grooß, J.-U., von Hobe, M., Strohm, F., Sumińska-Ebersoldt, O., Volk, C. M., Hösen, E., Mitev, V., Shur, G., and Müller, R.: Heterogeneous chlorine activation on stratospheric aerosols and clouds in the Arctic polar vortex, *Atmos. Chem. Phys.*, 12, 11095–11106, doi:10.5194/acp-12-11095-2012, 2012.
- Winker, D. M., Vaughan, M. A., Omar, A. H., Hu, Y., Powell, K. A., Liu, Z., Hunt, W. H., and Young, S. A.:
1020 Overview of the CALIPSO mission and CALIOP data processing algorithms, *J. Atmos. Ocean. Tech.*, 26, 2310–2323, 2009.
- ~~WMO: Scientific assessment of ozone depletion: 2006, Global Ozone Res., and Monit. Proj. Rep. 50, Geneva, Switzerland, 2007.~~
- ~~WMO: Scientific assessment of ozone depletion: 2010, Global Ozone Res., and Monit. Proj. Rep. 52, Geneva, Switzerland, 2011.~~
1025

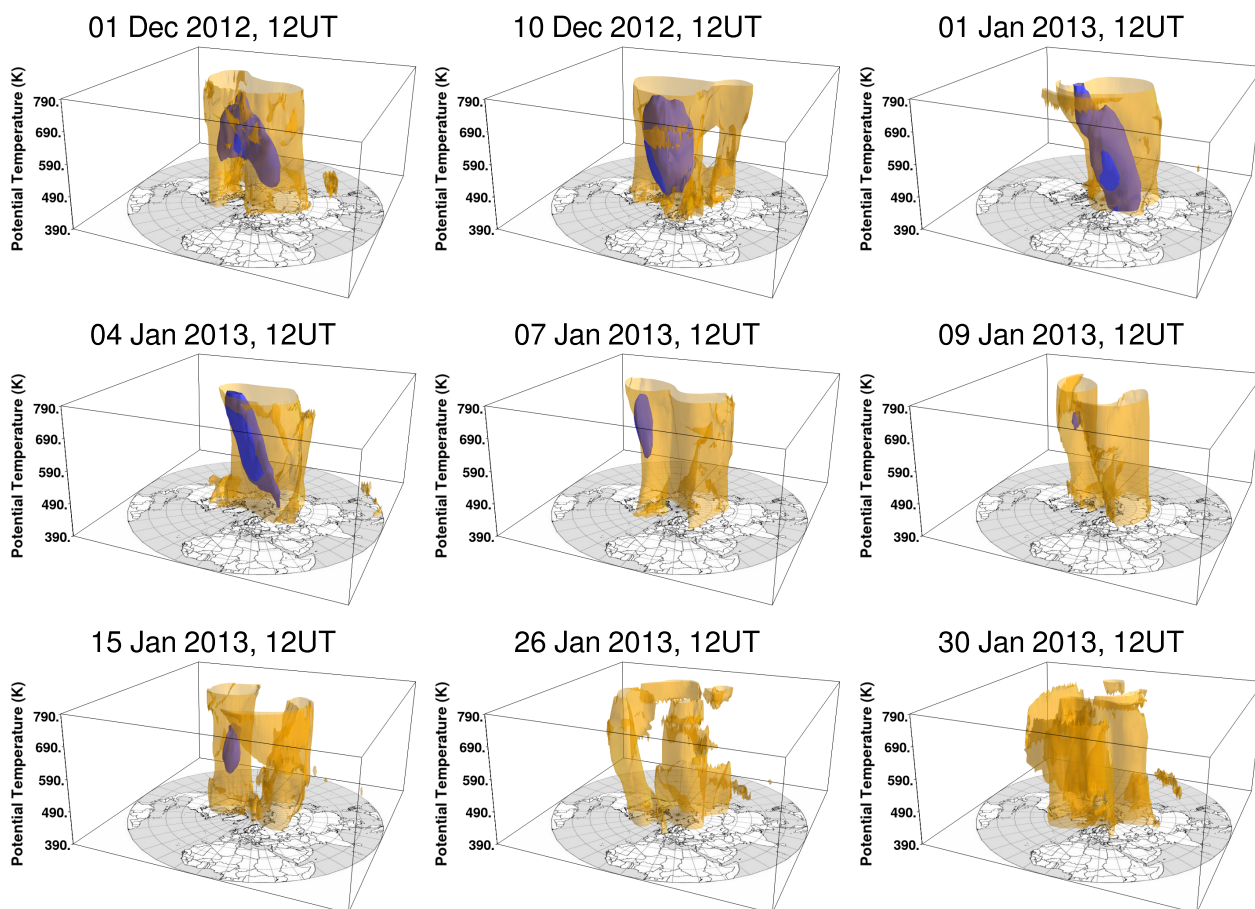


Figure 1. Isosurfaces of T_{NAT} (blue) and the vortex edge (orange). The vortex edge is defined by the altitude-dependent sPV profile described in Sect. 2.3.1. An animation covering the 2012/13 winter is available as a Supplement.

WMO: Scientific assessment of ozone depletion: 2014, Global Ozone Res., and Monit. Proj. Rep. 55, Geneva, Switzerland, 2014.

1030 Wohltmann, I., Wegner, T., Müller, R., Lehmann, R., Rex, M., Manney, G. L., Santee, M. L., Bernath, P., Sumińska-Ebersoldt, O., Stroh, F., von Hobe, M., Volk, C. M., Hösen, E., Ravagnani, F., Ulanovsky, A., and Yushkov, V.: Uncertainties in modelling heterogeneous chemistry and Arctic ozone depletion in the winter 2009/2010, *Atmos. Chem. Phys.*, 13, 3909–3929, doi:10.5194/acp-13-3909-2013, 2013.

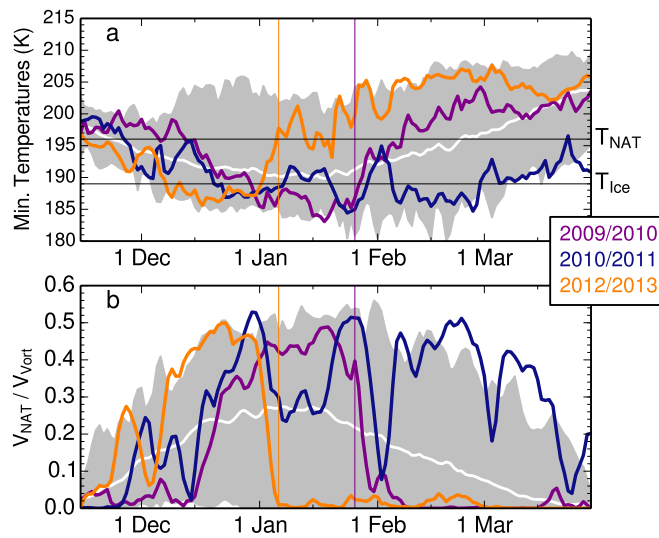


Figure 2. Time series of **(a)** minimum temperatures poleward of 40° N at 490 K and **(b)** $V_{\text{NAT}}/V_{\text{Vort}}$ (see text) from MERRA reanalysis. Individual lines show 2009/10 (purple), 2010/11 (blue) and 2012/13 (orange). Envelope shows the remaining years from 1979/80 through 2013/14. Thin vertical lines indicate the dates when the major SSW criteria were met in 2010 (purple) and 2013 (orange). Thin black horizontal lines in **(a)** indicate the NAT and ice PSC thresholds.

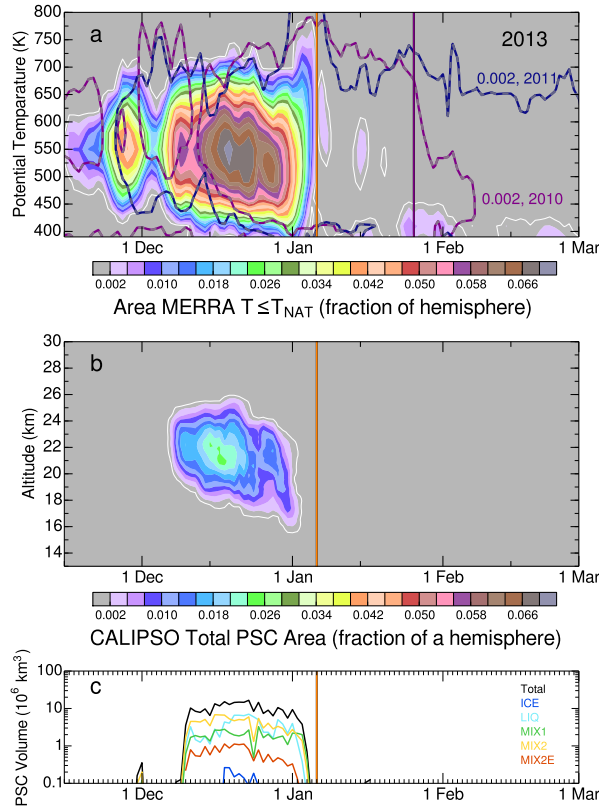


Figure 3. (a) Time series of the area poleward of 30° N with $T \leq T_{\text{NAT}}$ as a function of potential temperature in 2012/13 from MERRA (color fill; the white contour shows a value of 0.001, indicating a very small non-zero value); area is expressed as fraction of a hemisphere. The overlaid purple and blue contours show the 0.002 contour (which is at the boundary between grey and lavender in 2012/13) in 2009/10 and 2010/11, respectively; purple and orange vertical lines show the beginning dates of the SSWs in 2010 and 2013, respectively. (b) Time series of CALIPSO total PSC area; format is as in (a), but with only 2012/13 values. (c) Time series of the total volume of different types of PSCs observed by CALIPSO in 2012/13 (see text).

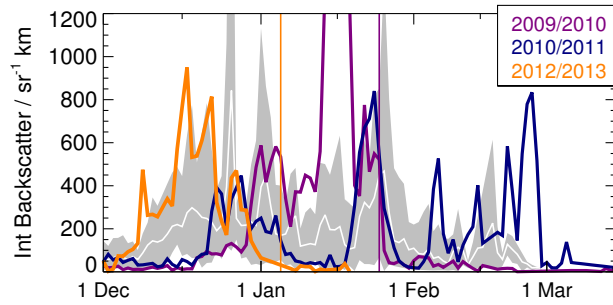


Figure 4. Vortex-integrated CALIPSO backscatter ($\text{sr}^{-1} \text{ km}$) at 490 K, proportional to the total liquid particle surface area within the vortex, as a function of day in 2012/13 (orange), 2010/11 (blue), and 2009/10 (purple) compared with the range (grey shading) and average (white line) for the other years in 2006/07 through 2013/14.

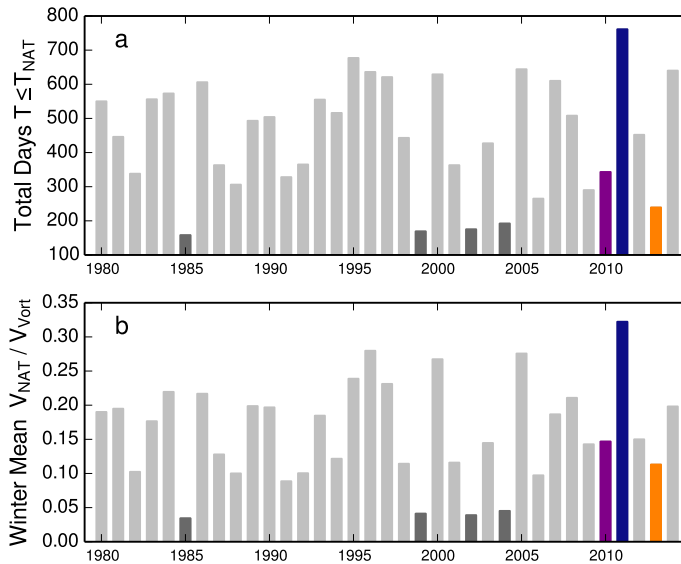


Figure 5. Summary temperature information from MERRA reanalysis for the past 35 Arctic winters: **(a)** the number of days below T_{NAT} summed over isentropic levels from 390 to 550 K; **(b)** winter mean $V_{\text{NAT}}/V_{\text{vort}}$ calculated from 1 December through 15 April. 2009/10, 2010/11, and 2012/13 are highlighted in purple, blue, and orange, respectively. Dark grey bars indicate other winters with major SSWs in December or early January. Year numbers are for the January of each winter.

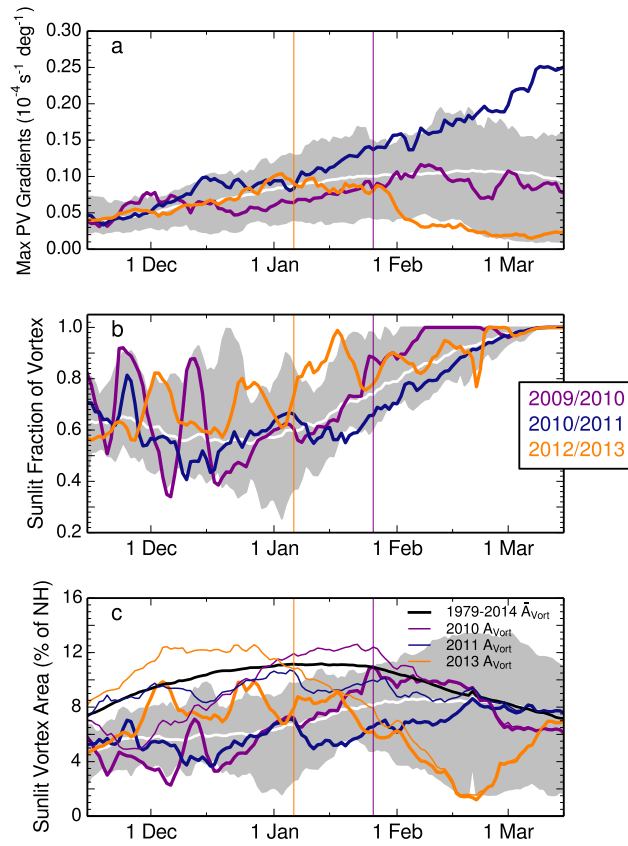


Figure 6. Time series from MERRA reanalysis at 490 K of (a) potential vorticity (PV) gradients as a function of EqL ($10^{-4} \text{ s}^{-1} \text{ deg}^{-1}$) and sunlit vortex area (SVA) expressed as (b) a fraction of the total vortex area and (c) a fraction of the hemisphere, with total vortex area shown as thin lines. Shading and line colors are as in Fig. 2.

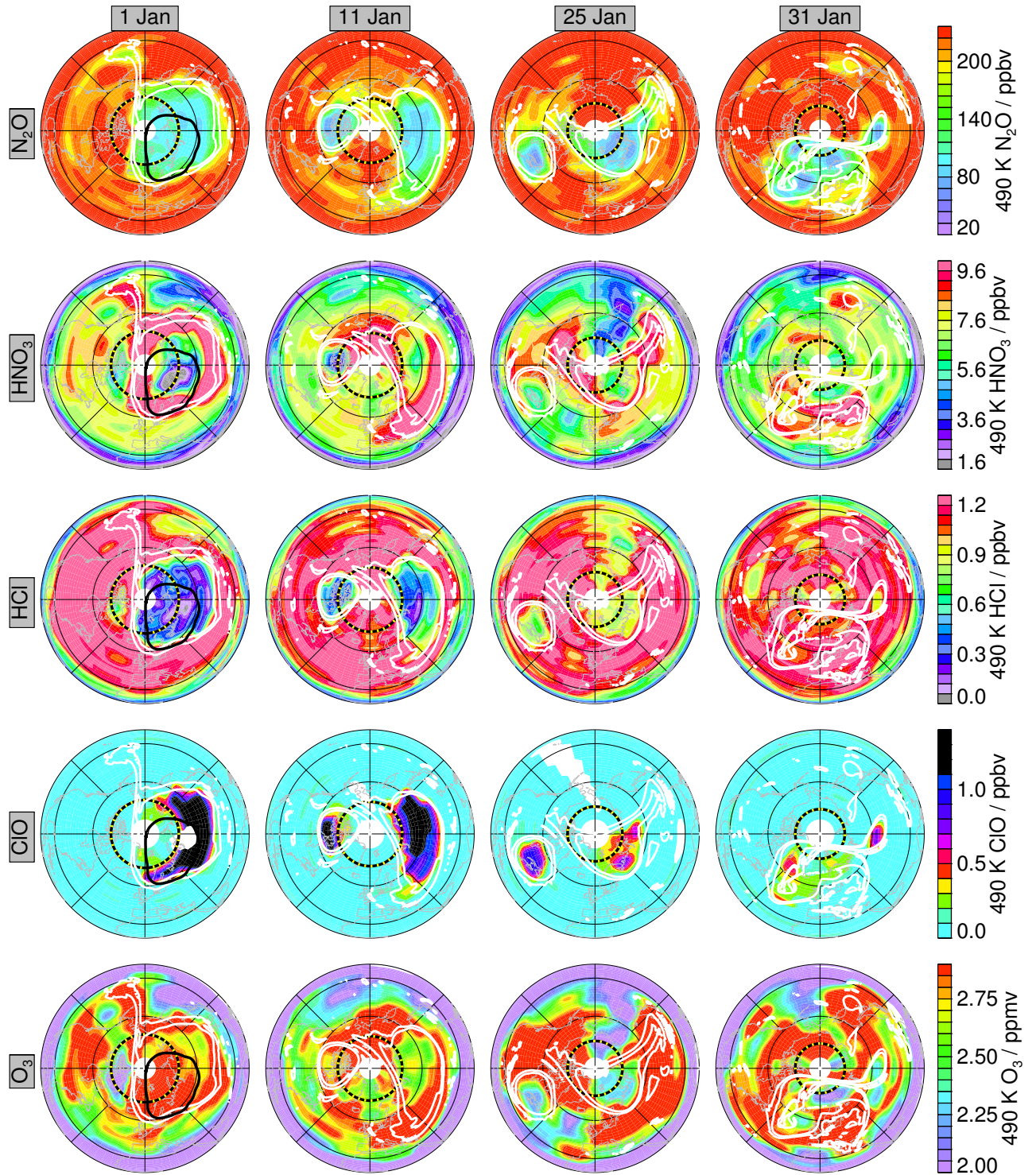


Figure 7. Maps of MLS trace gases on the 490 K isentropic surface for selected days in January 2013, top to bottom: N₂O (ppbv), HNO₃ (ppbv), HCl (ppbv), ClO (ppbv), and O₃ (ppmv). Yellow/black dashed line shows the latitude of polar night. White overlays are sPV contours of 1.2 and $1.6 \times 10^{-4} \text{ s}^{-1}$, representative of the vortex edge. The thick black contour (visible only on 1 January) outlines the region with temperatures less than 196 K, the approximate chlorine activation threshold. Projection is orthographic, with 0° longitude at the bottom and 90° E to the right. Thin black circles show 30 and 60° N latitudes.

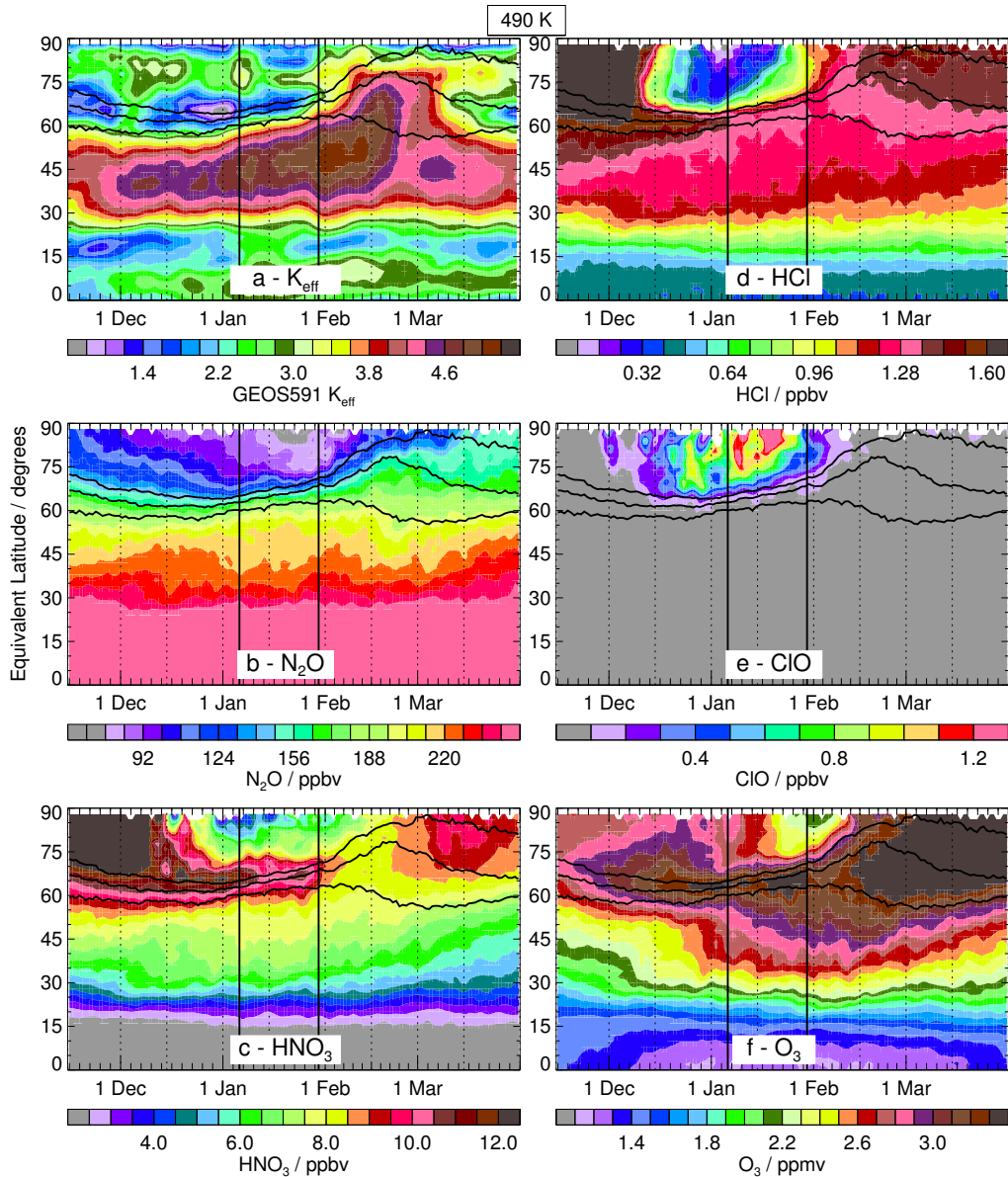


Figure 8. Equivalent latitude/time series at 490 K of (a) effective diffusivity from GEOS591 (expressed as log-normalized equivalent length; low values indicate transport barriers and high values regions of enhanced mixing) and MLS (b) N_2O , (c) HNO_3 , (d) HCl , (e) ClO , and (f) O_3 . Black contours show sPV values of 1.2 , 1.4 , and $1.6 \times 10^{-4} \text{ s}^{-1}$, in the vortex edge region. The thin solid black vertical lines indicate the onset day of the SSW (6 January, ~ 2 days before the vortex split) and the day when the offspring vortices reunited (30 January)

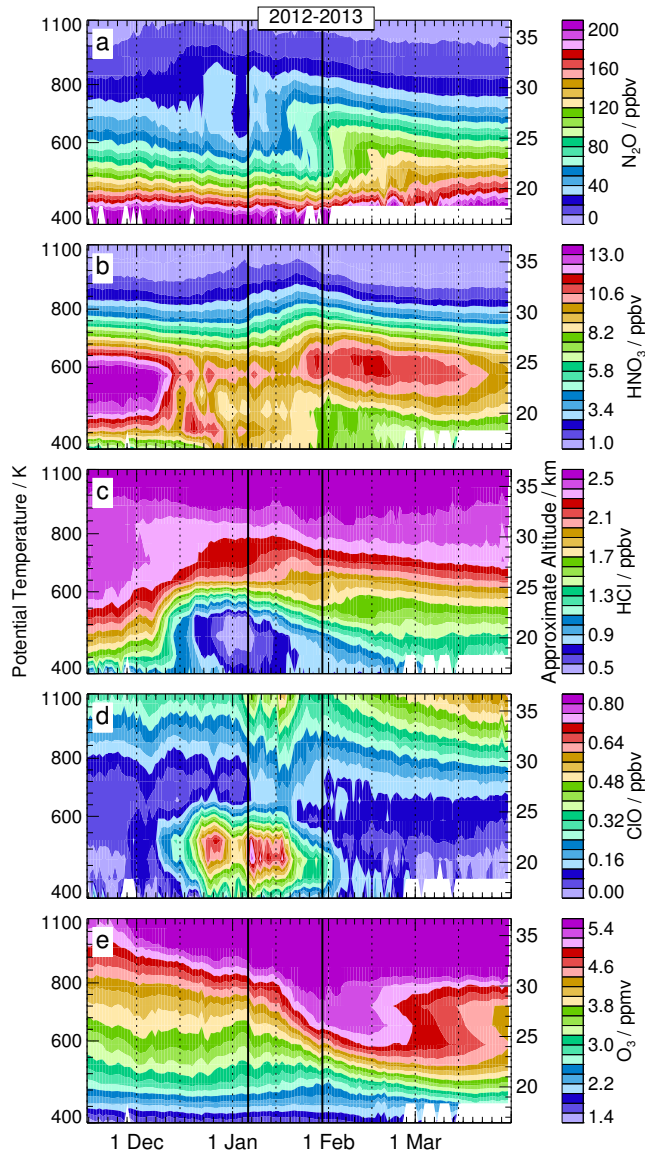


Figure 9. Potential temperature/time series of vortex averaged (within the $1.4 \times 10^{-4} \text{ s}^{-1}$ sPV contour) (a) N_2O , (b) HNO_3 , (c) HCl , (d) ClO , and (e) O_3 derived from MLS data. The thin solid black vertical lines indicate the onset day of the SSW (6 January, ~ 2 days before the vortex split) and the day when the offspring vortices reunited (30 January).

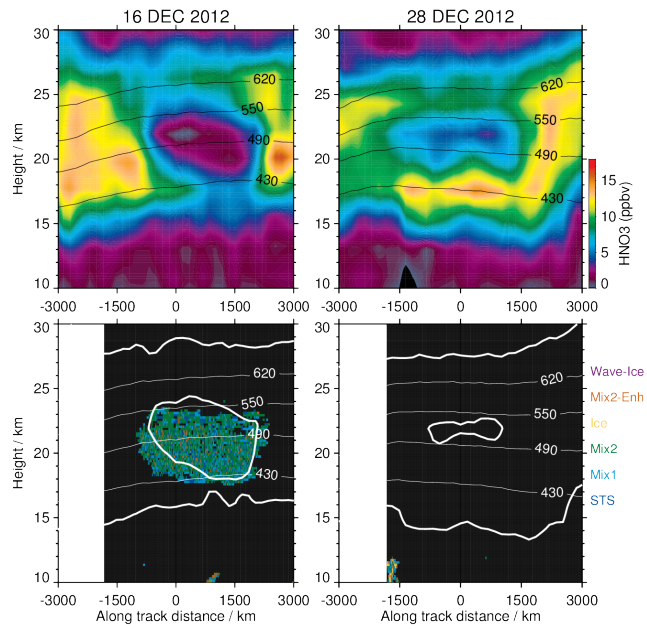


Figure 10. MLS HNO₃ (ppbv) along an orbit track (top panels) and colocated CALIPSO PSC classification (bottom panels, see text), on 16 and 28 December 2012. The orbit tracks shown on each day are very close to the same position and orientation, extending over Iceland approximately parallel to the easternmost part of the Greenland coast. The zero point on the tracks is at the turnaround of the orbit, that is, the point closest to the pole. Overlaid labeled lines are potential temperature contours. Overlaid thick white contour in the bottom panels is the 5 ppbv HNO₃ contour.

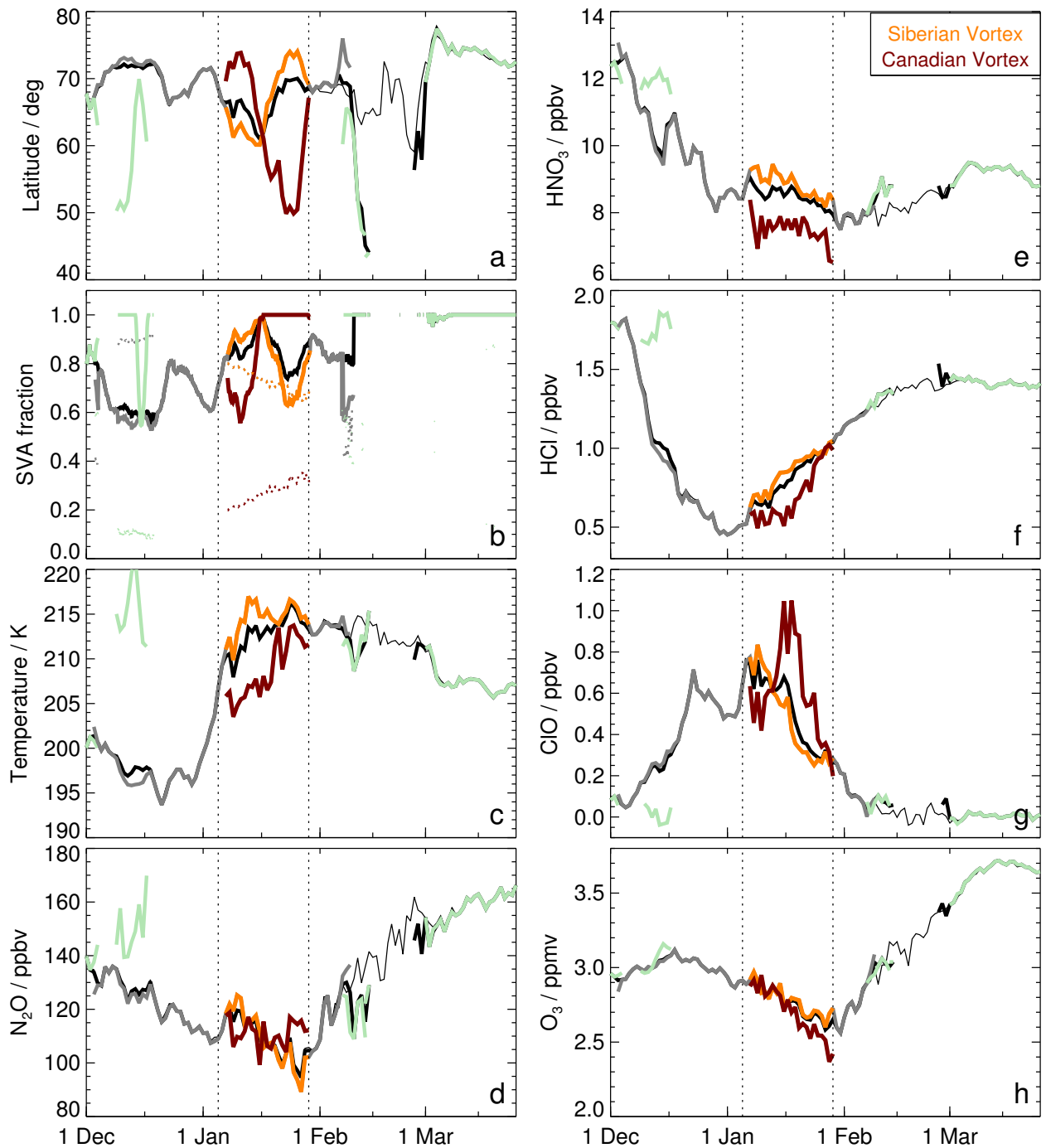


Figure 11. Characteristics of individual offspring vortices in 2012/13 at 490 K: **(a)** vortex-averaged latitude (degrees), **(b)** SVA expressed as a fraction of the vortex area (fine dotted lines show the fraction of total vortex area in each offspring vortex), vortex-averaged MLS **(c)** temperature, **(d)** N_2O , **(e)** HNO_3 , **(f)** HCl , **(g)** ClO , and **(h)** O_3 . Thick black lines show the fields for the sum over all vortices with area greater than 1 % of a hemisphere; thin black lines in vortex-averaged plots show “bulk” average (including individual regions with area less than 1 % of the hemisphere). Individual vortices are shown as thick grey and colored lines, with the “Siberian” and “Canadian” vortices in January shown in orange and dark red, respectively, and smaller offspring vortices at other times in light green. Thin vertical dotted lines are on 6 January (the onset of the major SSW, ~ 2 days before the vortex split) and 30 January (when the offspring vortices merged).

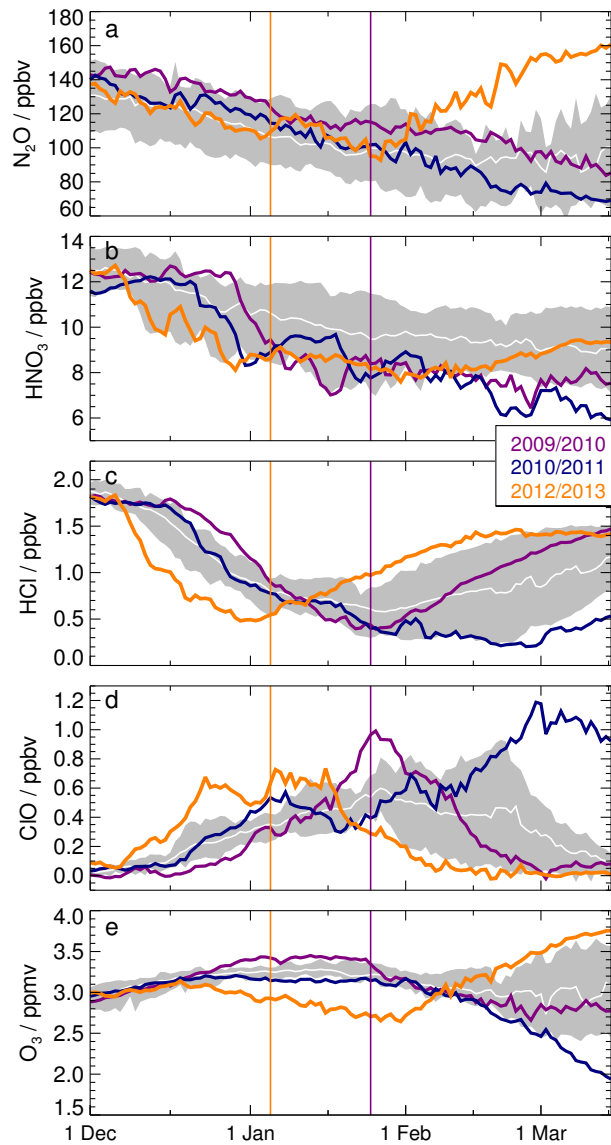


Figure 12. Vortex averaged MLS trace gases at 490 K, in 2012/13 (orange), 2010/11 (blue), and 2009/10 (purple) compared with the range (grey shading) and average (white line) for the other [years-Arctic winters](#) in 2004/05 through 2013/14. **(a)** N_2O , **(b)** HNO_3 , **(c)** HCl , **(d)** ClO , and **(e)** O_3 . Vertical purple and orange lines show the onset dates of the SSWs in 2010 and 2013, respectively.

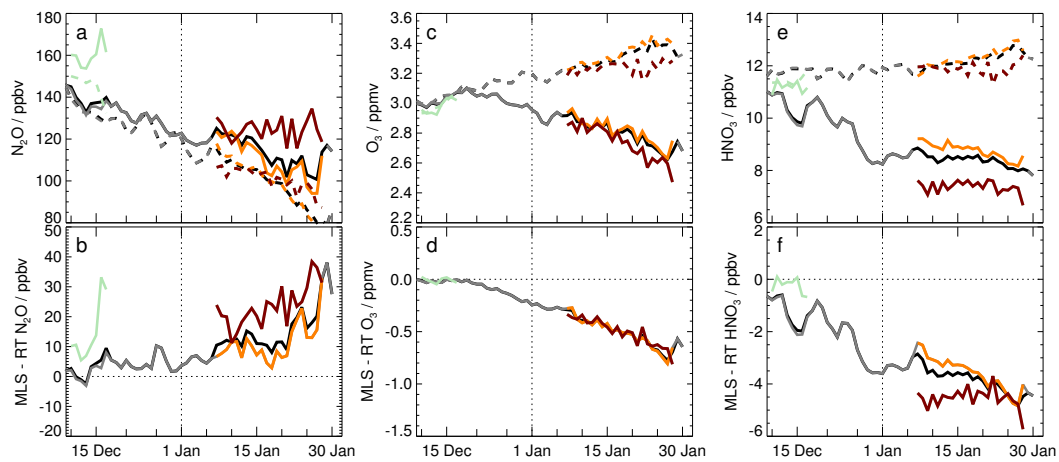


Figure 13. Vortex-averaged (left to right) N_2O , O_3 , and HNO_3 from MLS (solid lines) and RT passive subtraction (dashed lines) calculations (see text) at 490 K from 8 December 2012 through January 2013. (a), (c), and (e) show mixing ratios in each of the vortices present; (b), (d), and (f) show the difference between MLS and RT (passively transported) values, indicative of transport uncertainties for N_2O , and chemical and/or microphysical changes for O_3 and HNO_3 . Line colors are as in Fig. 11.

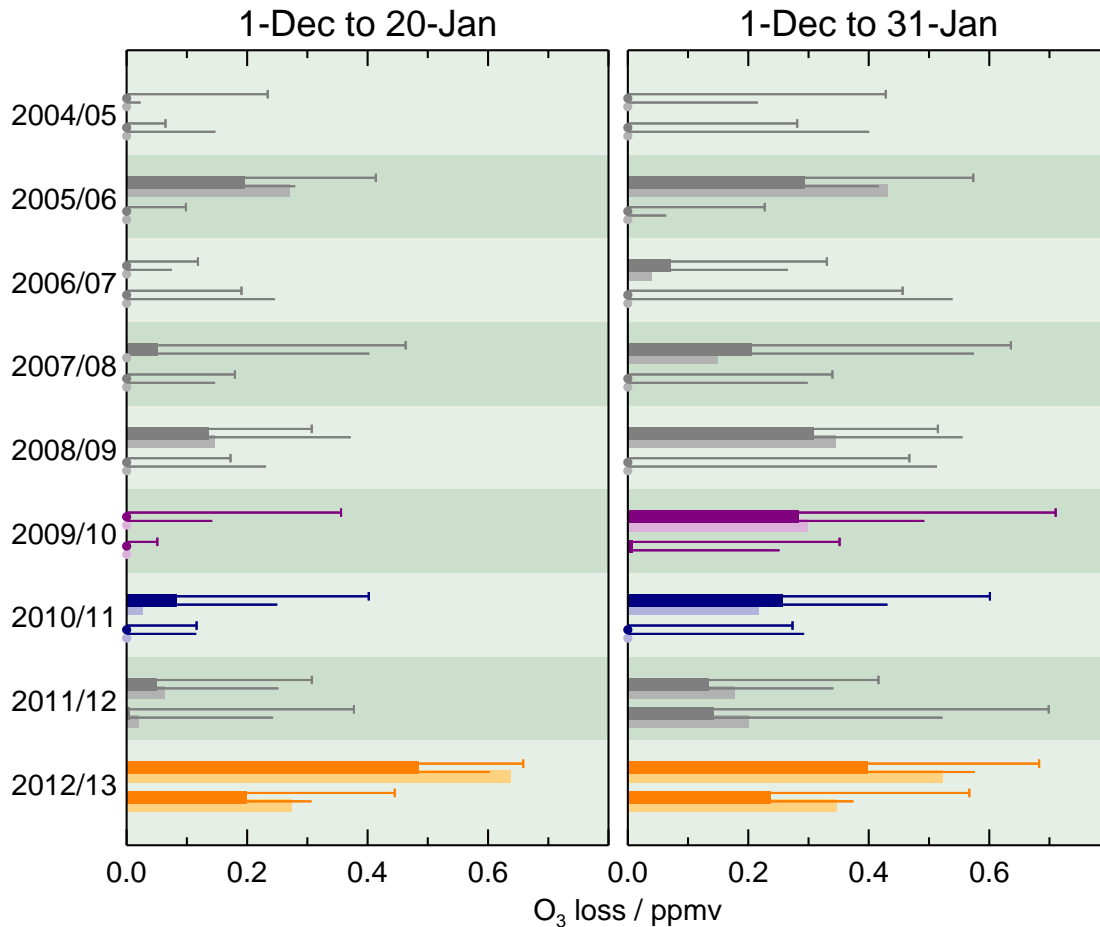


Figure 14. Chemical ozone loss estimates for 1 December through (left) 20 January and (right) 31 January from MLS Match (Livesey et al., 2015) for the 2004/05 through 2012/13 Arctic winters. Integrated ozone loss for each Arctic early winter, in 25 K potential temperature bins centered at 500 K (top bar of pair for each year) and 450 K (bottom bar of each pair), is shown as wide bars, with overlapping wide pale bars showing the calculations using “stricter” match requirements (see Sect. 2.3.3). Dots on the left hand axis indicate where the estimated ozone change was zero or positive, indicating no chemical loss. Thin lines extending to the right of the wide bars show uncertainties in ozone calculated assuming N_2O changes are ascribed to errors in descent (upper lines, with “tails” at right hand end) or mixing across the vortex edge (lower lines, with no tails). As in previous figures, 2009/10, 2010/11, and 2012/13 are highlighted in purple, blue, and orange, respectively.

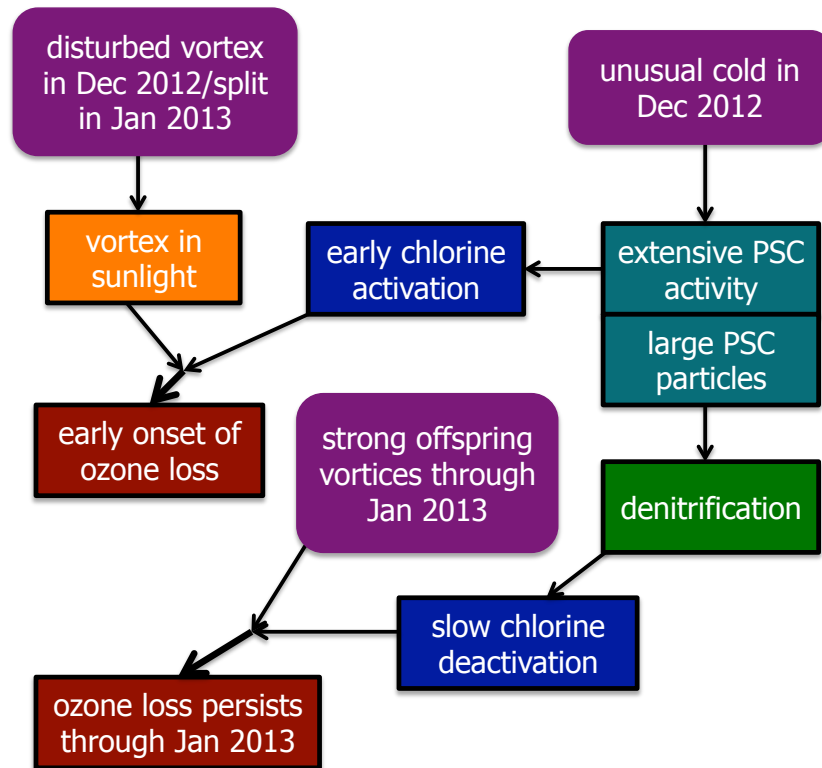


Figure 15. Block diagram of the processes leading to unusual early winter chemical ozone loss in 2012/13. Purple boxes show the key dynamical processes that, in combination, resulted in the unusual early winter chemical processing. Blue-green and blue boxes show PSC and chlorine processes, respectively. Orange box indicates sunlight exposure and green box denitrification. Both phenomena going into each dark red box were necessary for the chemical ozone loss to take place.